068670-12-P C00-1407-55

College of Engineering
Department of Atmospheric and Oceanic Science

Progress Report No. 10

RAIN SCAVENGING STUDIES

A. Nelson Dingle

U.S. Atomic Energy Commission
Contract No. AT(11-1)-1407
Argonne, Illinois

July 1974

LIST OF FIGURES

TABLE OF CONTENTS

LIST OF FIGURES (continued)

ABSTRACT

Studies conducted over the last few years on the observations and measurements made in the field on 1 June 1970 are assembled and interpreted in terms of the modelling of convective shower systems and their scavenging patterns. The modelling of cloud microphysics in relation to precipitation generation and scavenging as well as convective system dynamics is also discussed. It is suggested that parameterizations of the microphysical processes and the fine-scale dynamics will probably have to be tested for adequacy against nearly full scale computations in three dimensions using time-dependent equations with variable boundary conditions. Steps toward this long term objective are planned.

B. THE SAMPLING NETWORK

A. INTRODUCTION

The experiment described here is a sequel to the 1967 pilot experiment (Dingle, et al, 1969). It was designed for a twofold purpose: (1) to observe the behavior of a convective storm in terms of its redistribution of a fine particle tracer placed in its updraft by means of an aircraft burning pyrotechnic flares in a definite pattern, and (2) by analogy with the silver iodide pyrotechnic flare cloud-seeding procedure, to interpret the results in terms of their relevance to this weather modification technique. Our present objective is to interpret the results in terms of requirements of and useful information for improved numerical models of convective shower systems.

It is quite well understood that a particulate cloud rising in an updraft with sufficient water vapor will become associated with or attached to cloud and rain water and will be deposited in some proportion on the ground. The scavenging processes of importance are (1) nucleation of cloud droplets upon particles of at least 0.2μm radius, (2) collection of very small particles, less than about 0.03μm radius, on cloud droplets by diffusive processes, and (3) impact collection of relatively large particles (radius at least 2μm) by falling raindrops. (See, e.g., Greenfield, 1957; Fletcher, 1962; Junge, 1963). All of these processes should operate on a plume of silver iodide particles just as they do on a plume of indium-labeled smoke or any other material having similar physical properties.

B. THE SAMPLING NETWORK

The central Illinois network of the Illinois State Water Survey (ISWS) is a grid of recording raingauges spaced about 4.8 km apart on the average and covering a square of 3880 km^2. The need for such a base for the experiment is apparent. For the tracer experiment, about one-quarter of the entire network, was selected and further instrumented.

The University of Michigan sampling net was superimposed in such a way as to reduce the sample grid spacing to about half that between raingauges (Fig. 1). On such a network, including the raingauge stations, whole-storm samplers were set out prior to rain and picked up immediately after rain by teams of research assistants in mobile (auto-van) units. The whole-storm samplers were wide-mouthed (~50 cm diameter) buckets that were lined with polyethylene bags.

Sequential samples of rain were also collected at six different stations to provide temporal resolution of the tracer deposition in rain. Three of these (M, M1, M2, Fig. 2a) were operated manually by the field crew, and three (G1, G2, G3, Fig. 2a) were electrically operated automatic units supplied by Argonne National Laboratory (Gatz, et al, 1971).

C. THE EXPERIMENT, CONDITIONS AND RESULTS

On 1 June 1970 a line of thunderstorms and showers associated with a cold frontal system approached the network from the west. Details of the experimental design have been presented

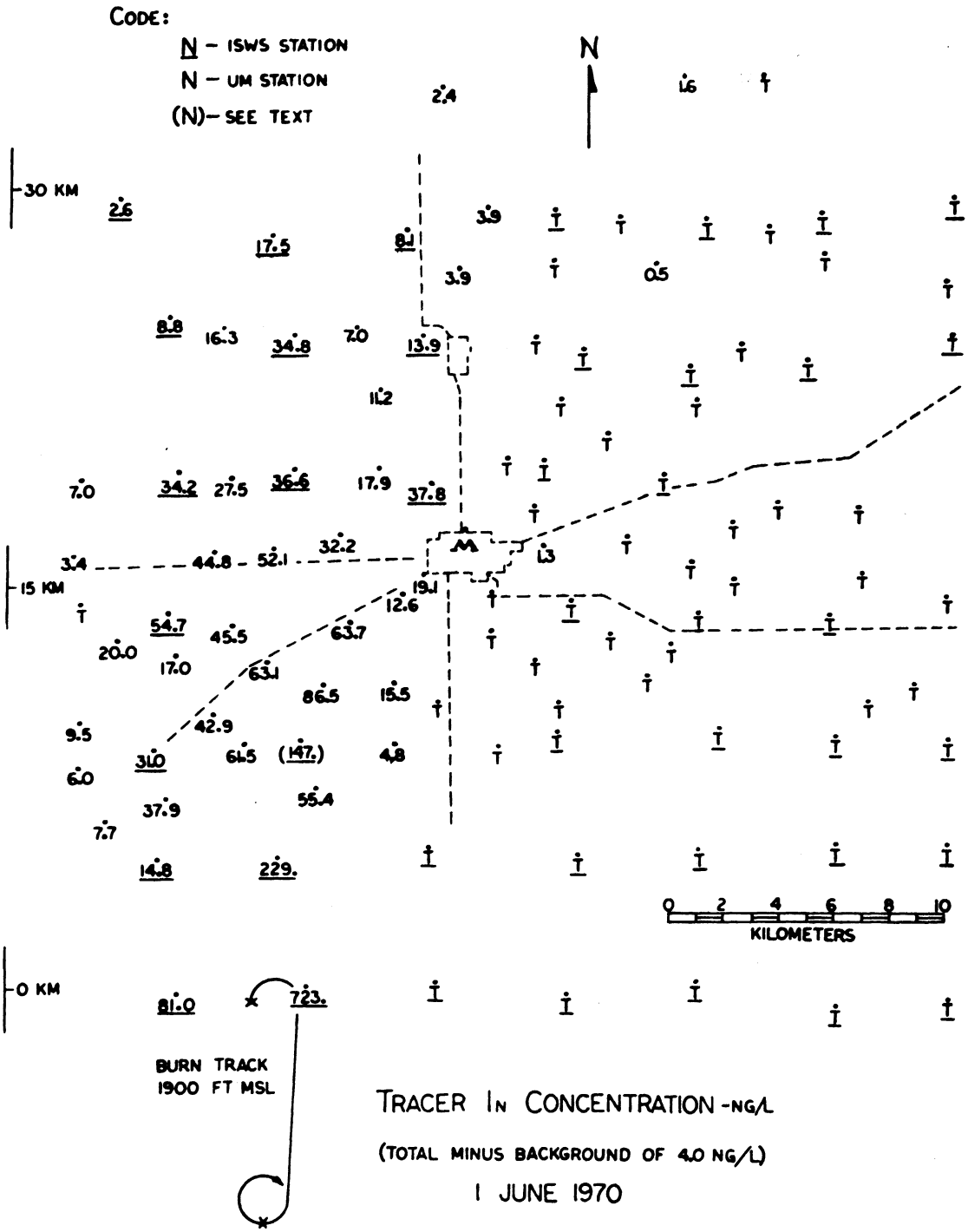

Figure 1. The sampling network showing the burn track and indium concentrations in ng l^{-1}

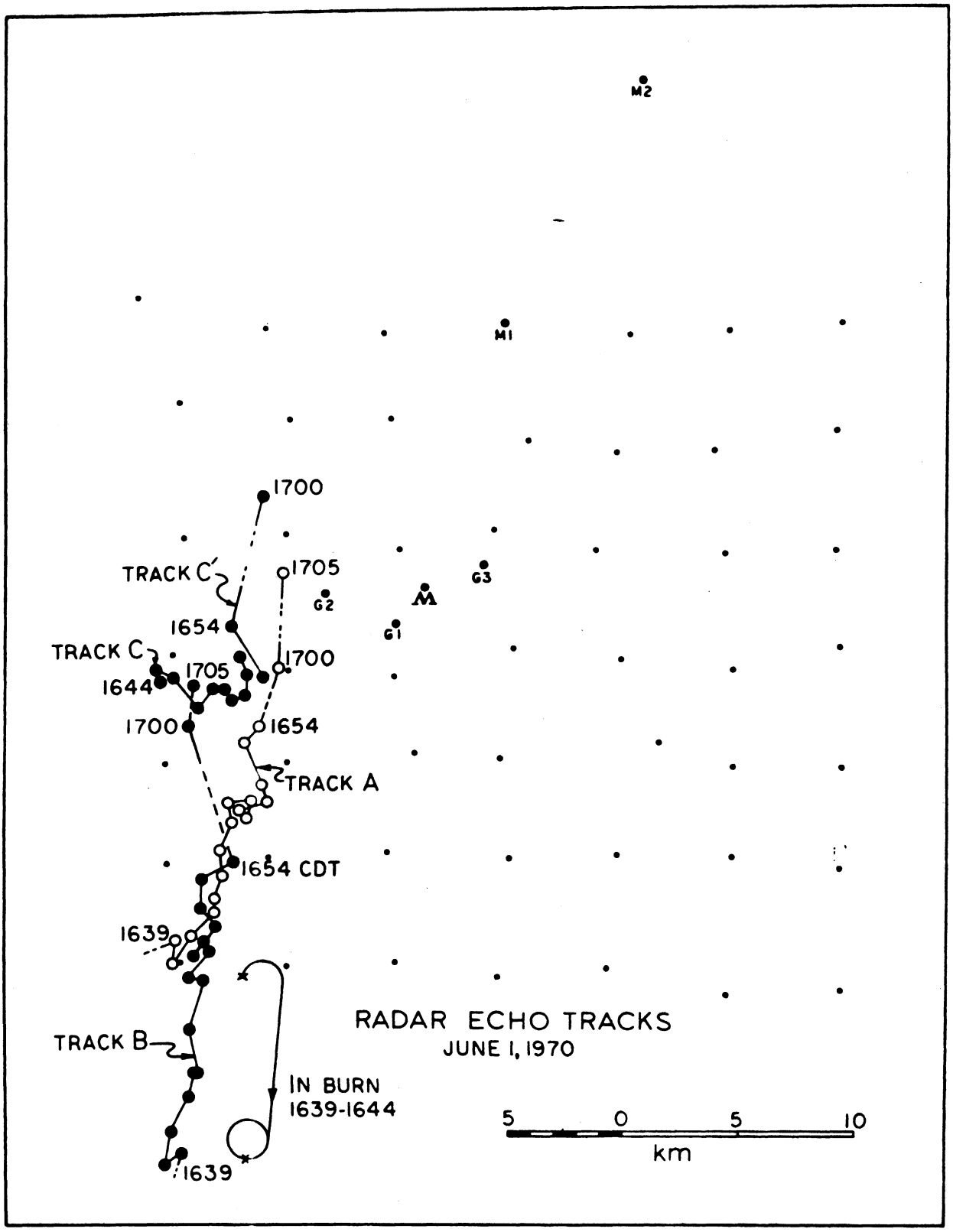

Figure 2a. Radar echo centroid positions relative to the burn track from 1639 to 1705 CDT

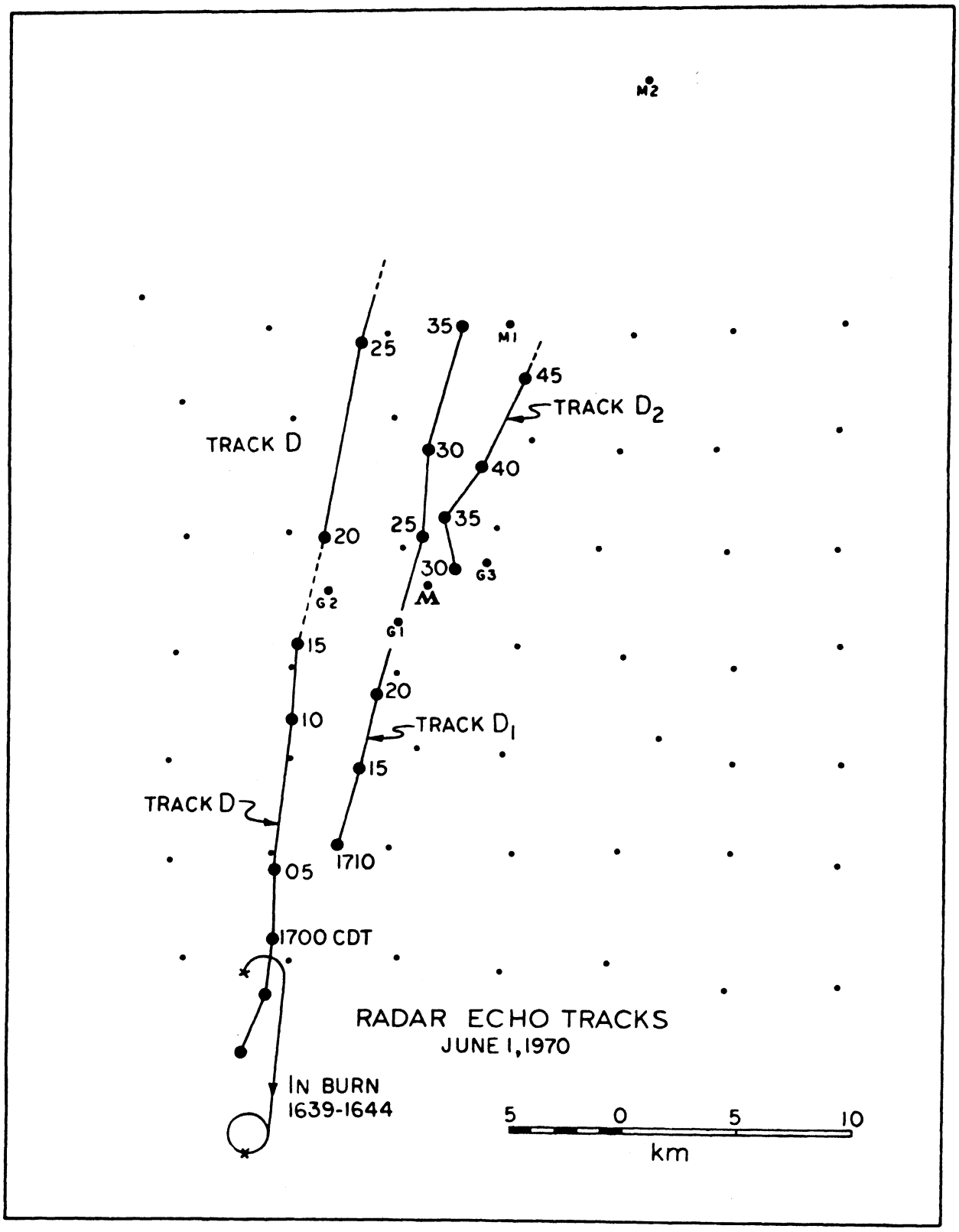

Figure 2b. Radar echo centroid positions relative to the burn track from 1650 to 1745 CDT

elsewhere (Dingle, 1970). Twelve pyrotechnic flares loaded with $In(OH)_3$ were burned simultaneously aboard an airplane flying about 400 m above the ground in updrafts feeding the convective cells. The burn path is shown in Figures 1 and 2. During the burn, the aircraft was below and ahead of the cloud bases, and the nearest rain was 2 to 3 km to the west. The burn path was about 16 km long from ignition to burnout. Radar echoes visible during the five-minute burn period are shown in Figure 2a. The radar echo locations for the later portion of the rain period are shown in Figure 2b.

1. Synoptic Situation.

The synoptic weather situation is shown by the sectional map constructed from hourly aircraft weather sequences for 1700 CDT (Figure 3). Available soundings are those from Peoria (PIA) and Salem (SLO), at 1900 CDT (Figures 4 and 5). These stations are respectively 85 km northwest and 168 km south of the network area (Figure 3). At Peoria the frontal inversion is about 0.25 km deep with its base at 3.5 km. Below this level, the air stratification is wet-super adiabatic down to 1.5 km, then wet adiabatic to 0.5 km and dry adiabatic to the surface. The winds are southerly at all levels except the lowest where a light north-northeast wind is observed. This light northerly wind drift characterizes the surface air flow to a considerable distance west of the front (Figure 3) with a somewhat stronger easterly component observed nearer the front and southwest of the network. It is evidently confined to the lowest 0.5 km or so despite the fact that the frontal inversion lies above 3.5 km at this place and time.

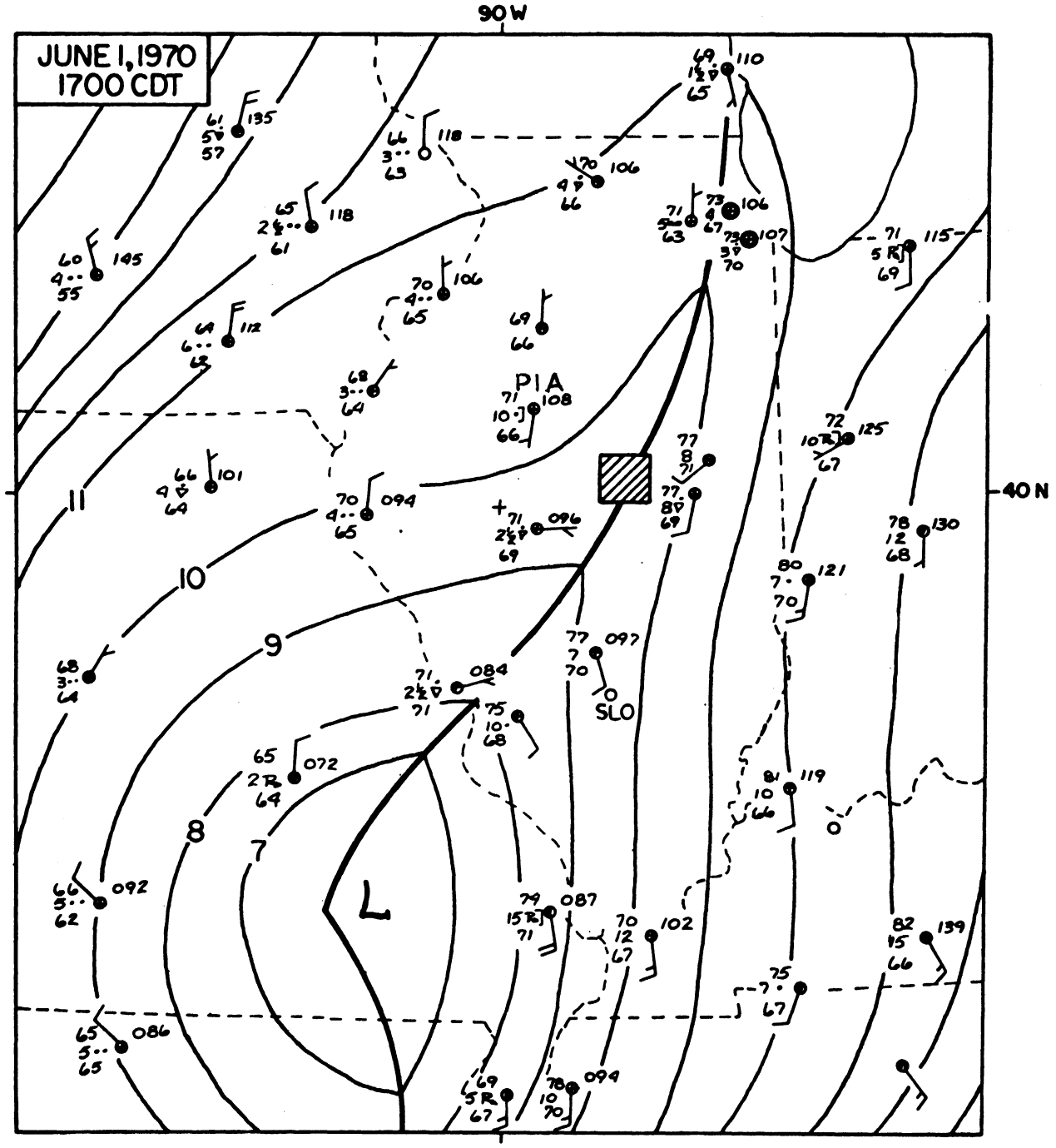

Figure 3. Sea level sectional weather map, 1700 CDT. Note locations of PIA and SLO. The hatched square is the network area.

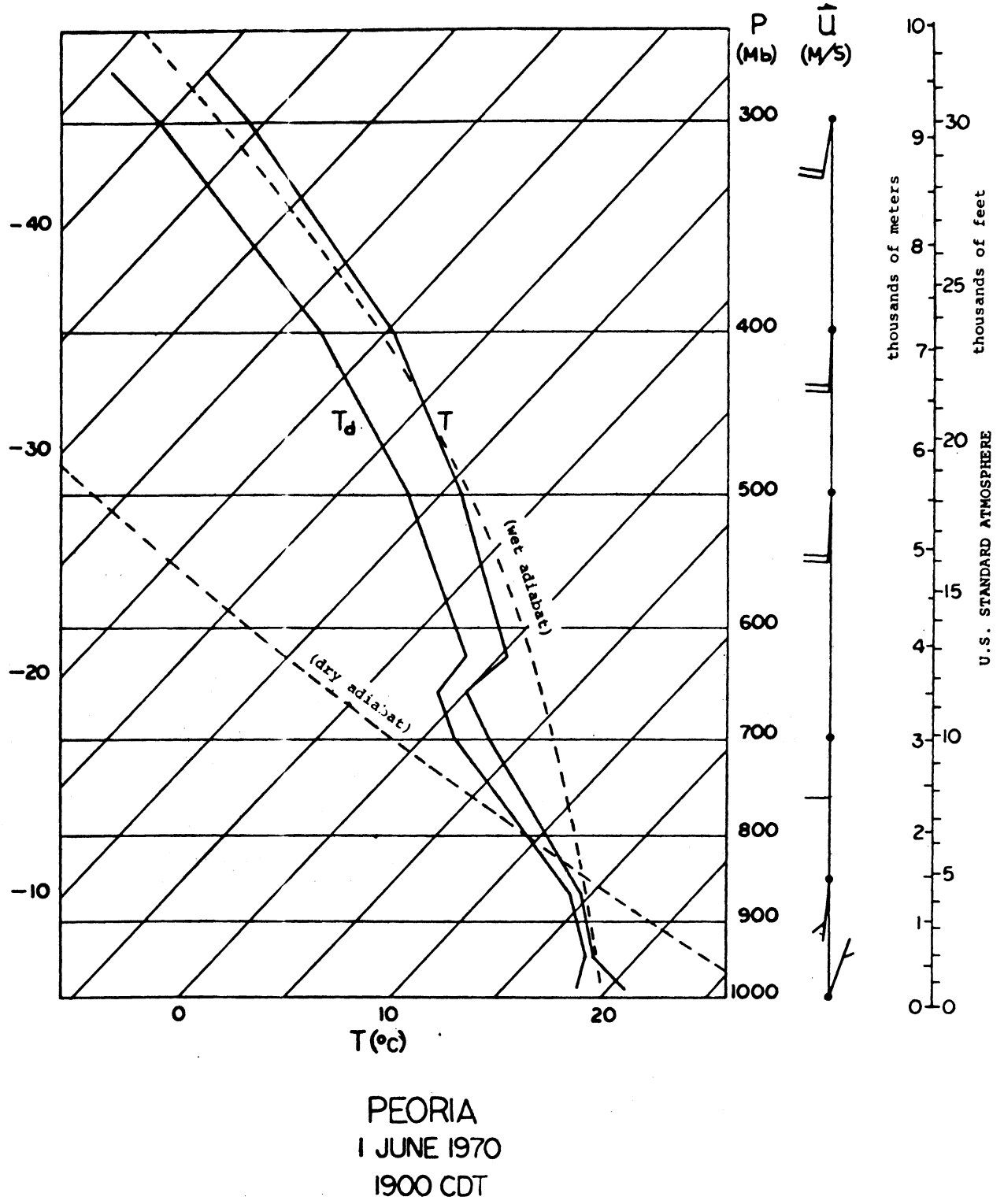

PEORIA
1 JUNE 1970
1900 CDT

Figure 4. Rawinsonde data for Peoria, Ill. (PIA), 1900 CDT

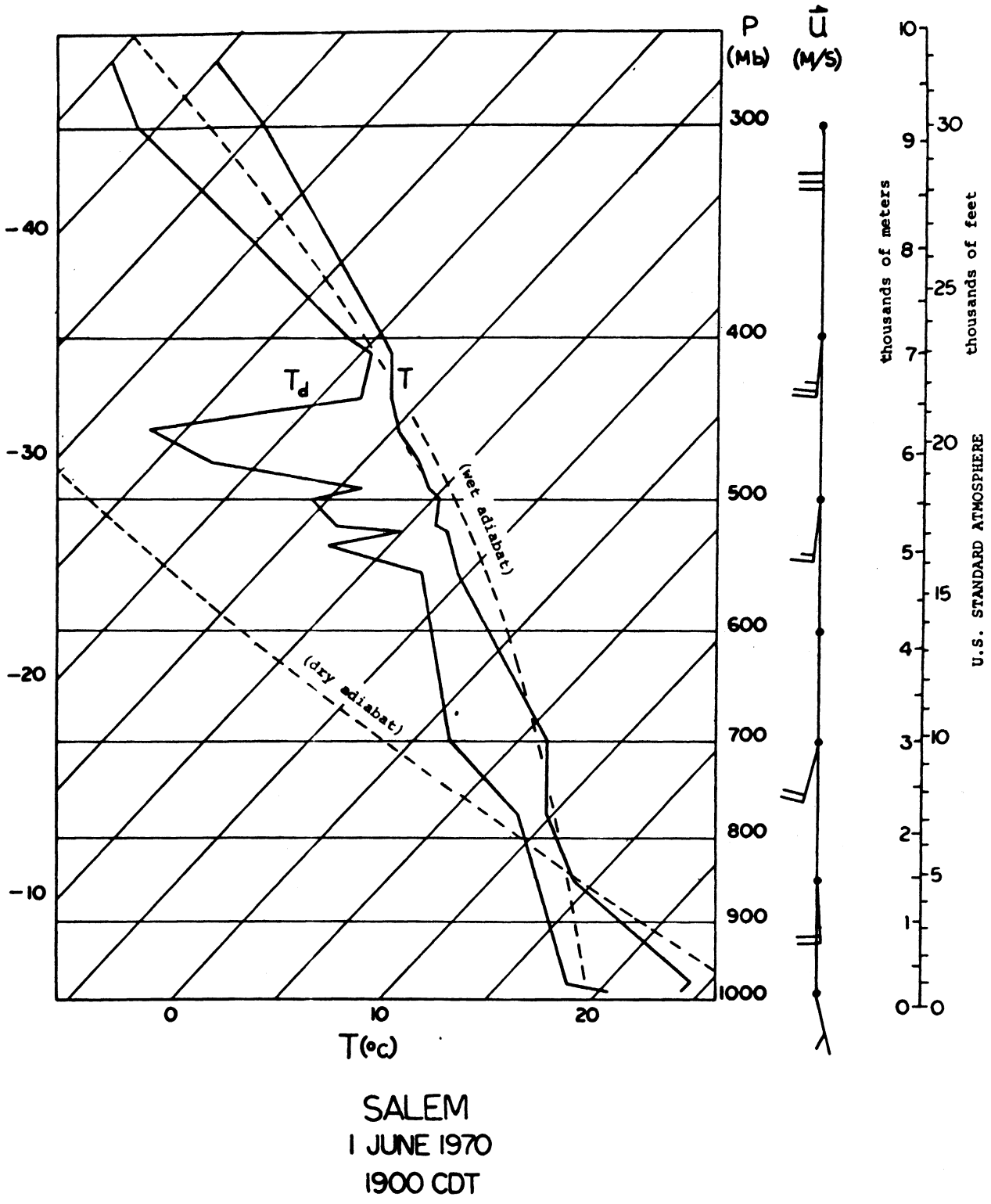

Figure 5. Rawinsonde data for Salem, Ill. (SLO), 1900 CDT

At Salem (Figure 5) the stratification is nearly wet adiabatic from 1.5 to 6.5 km, and slightly subadiabatic below 1.5 km. The warm air flow is southerly to the limit of the data at 9 km, with only the slightest easterly component below 1.5 km, and a somewhat stronger westerly component above that level to at least 7 km.

2. Tracer Deposition and Rainfall

As indicated above, tracer data were obtained by means of two different sampling systems, (1) an areally distributed network of whole-storm samplers, and (2) sequential samples collected at six stations.

a. Areal deposition patterns for tracer and rain.

The analysis of the rain samples for In content was done by neutron activation (Bhatki and Dingle, 1970). Deduction of background was done before computing deposition, and the limits of the deposition pattern were determined by the measured mean background concentration of 4 ng l^{-1}. The resulting In deposition pattern is shown in Figure 6. Isopleths are drawn at doubling intervals because an exponential decay pattern is nominally to be expected (Engelmann, 1968), and the common ratio 2 is easily handled. The close-packed parallel isopleths that form the eastern side of the pattern clearly indicate the atmospheric inflow region. Somewhat surprising, however, in view of the wind field and the explicit effort to place the tracer in an updraft area, at 400 m altitude east of the front is the westward spread of the tracer to the extent that the "5" isopleth, indicating 2^5 = 32 ng m^{-2} In deposition, is displaced beyond the western limit of the network. This suggests that the frontal

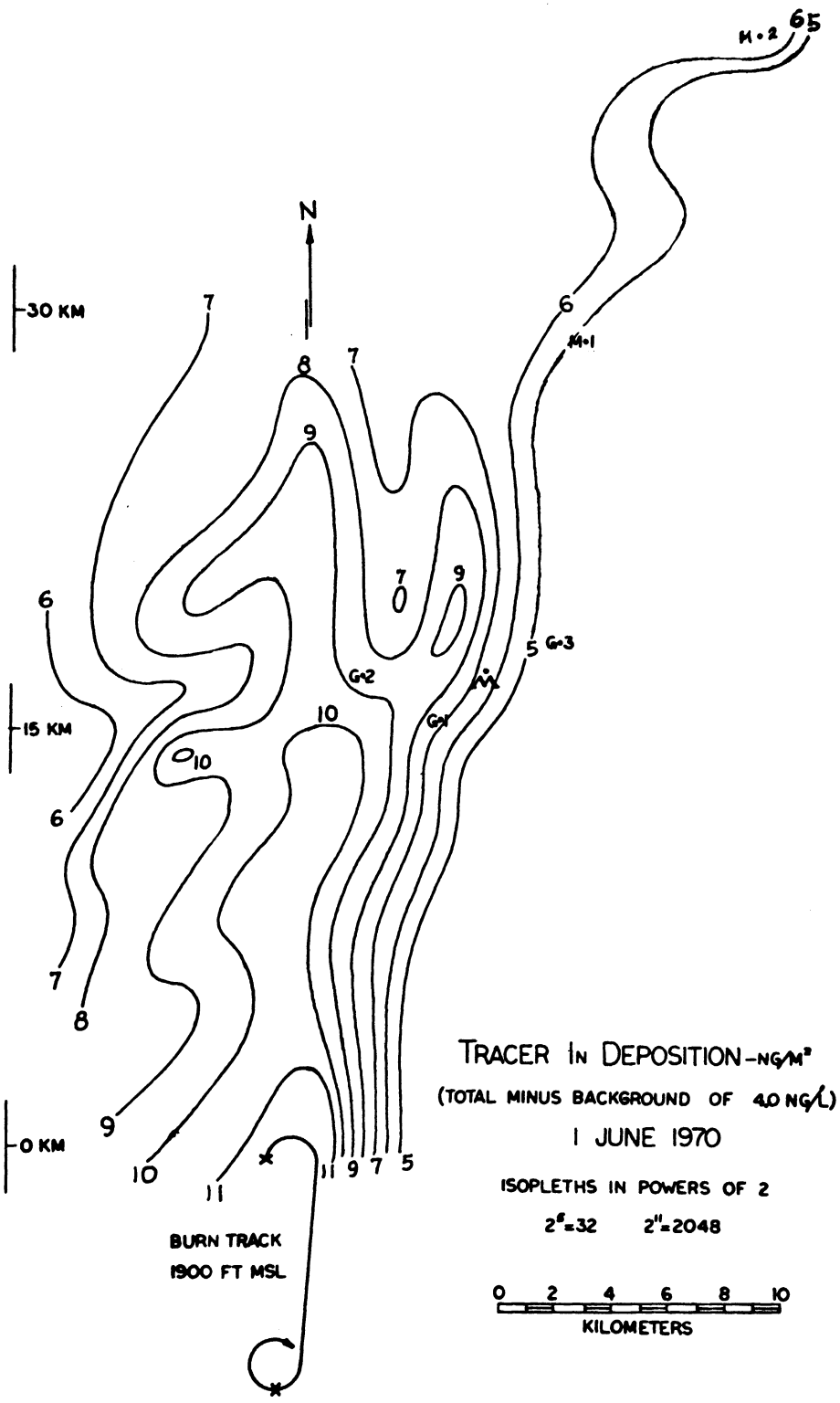

Figure 6. Pattern of deposition of indium tracer

structure is more complicated and the frontal surface is more permeable than is indicated by most meteorological models. The complications are directly attributable to the details of circulation imposed by the convective meso-systems.

The total rainfall for the 1 June 1970 rain event is shown in Figure 7. The disorganized pattern is typical of summer rains of the area and indicates a moderate intensity of the rain-producing system with local maxima ranging up to 3.5 cm, but most stations reporting less than 2 cm. Clearly this information is inadequate as a base for interpreting the tracer experiment. Inasmuch as the tracer emission was specifically timed and explicitly located, the spacial and temporal coincidence of the tracer plume and the rain source must be studied.

b. Temporal data for tracer and rain

The evolution and propagation of the rain system are indicated by several project information sources.

i. Aircraft and radar echo data.

According to the project aircraft crew, the cloud field was confused and disorganized prior to about 1630 CDT. Relatively better organized convection began to appear off the southwest corner of the network at about 1630. This better-organized convection produced the radar echoes A and B by 1639 (Figure 2a), and echo C by 1644. Echoes A and C were associated with more or less discrete and isolated showers. Echo B, however, appears to have been the first in the series B, D, D_1, D_2 (Figure 2a,b) composing a self-propagating series of moderate thunderstorms which cycled through these four generations until at least 1745 when the radar was shut down.

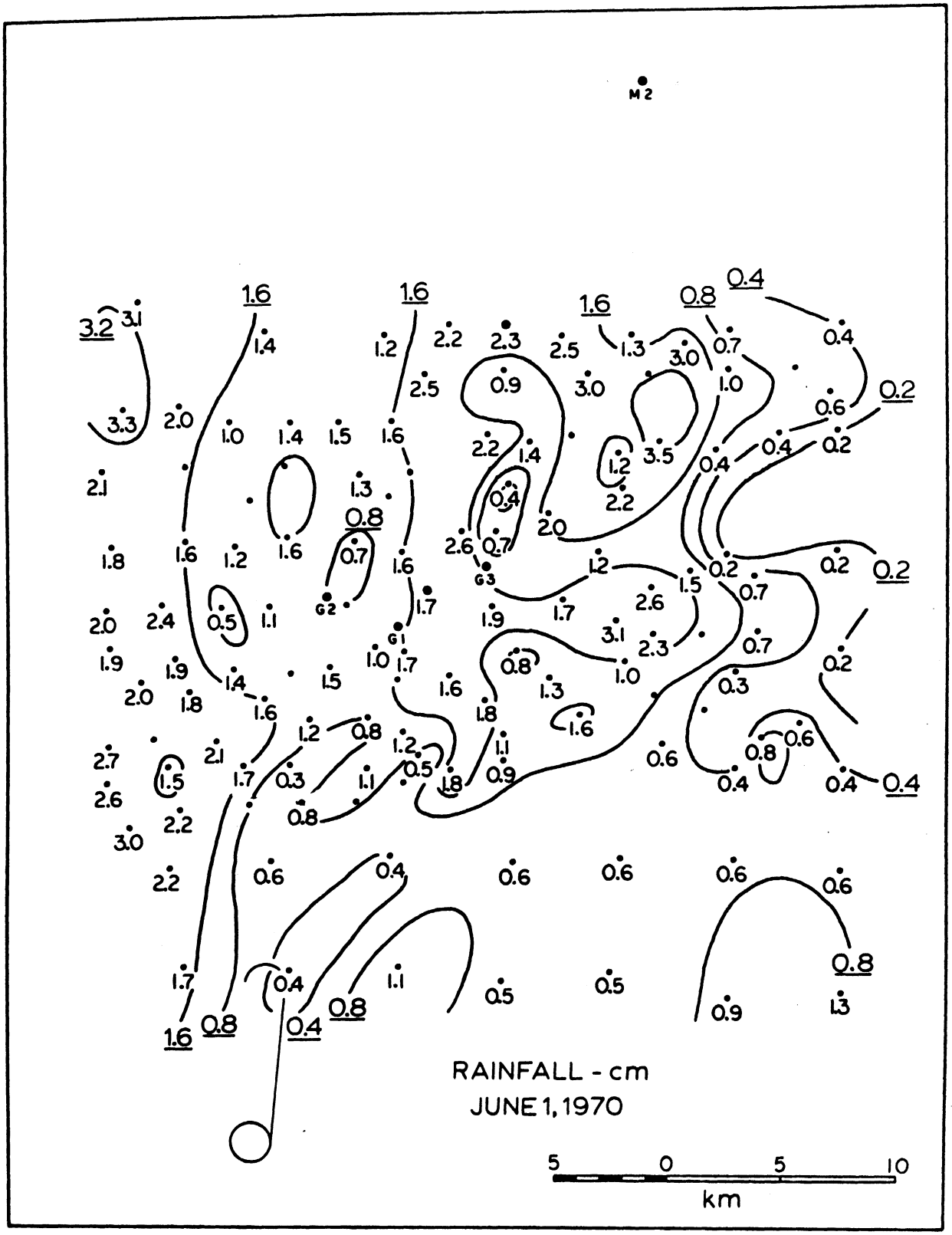

Figure 7. Total rainfall distribution from ISWS raingauge network

ii. Rainfall analysis.

The radar data yield only a part of the information required to explain the distribution of rainfall (Figure 7) and of tracer deposition (Figure 6). Further information was developed by analysis of the ISWS raingauge records. The rain accumulation was resolved by 10-minute intervals using the original records to derive two overlapping sequences, one covering the period 1620-1840 CDT and the other covering the five-minute-displaced period 1625-1845 CDT. The rain field propagation was derived from these by means of graphic overlays on which the successive positions of estimated shower centroids and the .08-, .16- and .32-in (12.2, 24.4, and 48.8 mm hr^{-1} average rainfall intensity, resp.) isohyets were plotted. The results (Figures 8a,b) indicate a series of seven more or less distinct shower systems over the network during the 1620-1845 CDT period. By contrast, apparently because of attenuation on the one hand and ground clutter on the other, the radar failed to show systems IV, V, and VI. The radar was shut down at 1745, before system VII appeared, partly because it was not expected that any of the tracer plume would be found within the network after 1745.

Evidently rain systems I, II, III can be identified with radar echoes A, B, C, and D (system I), D_1 (II), and D_2 (III). System IV is quite possibly a fifth generation of the self-propagating sequence, but it appeared after the radar had been shut down.

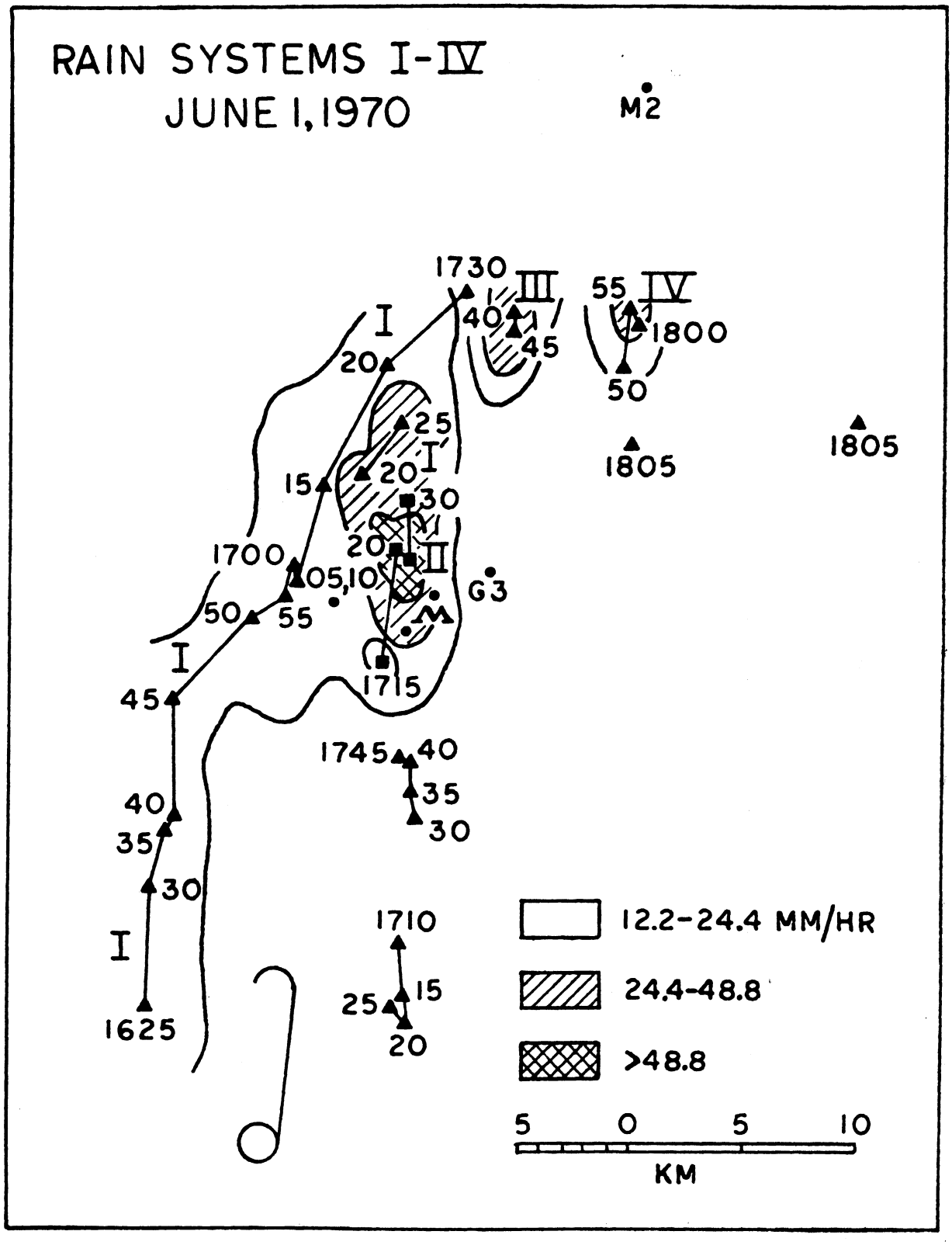

Figure 8a. Ten-minute isohyet envelopes for rain systems I through IV, 1620 to 1810 CDT

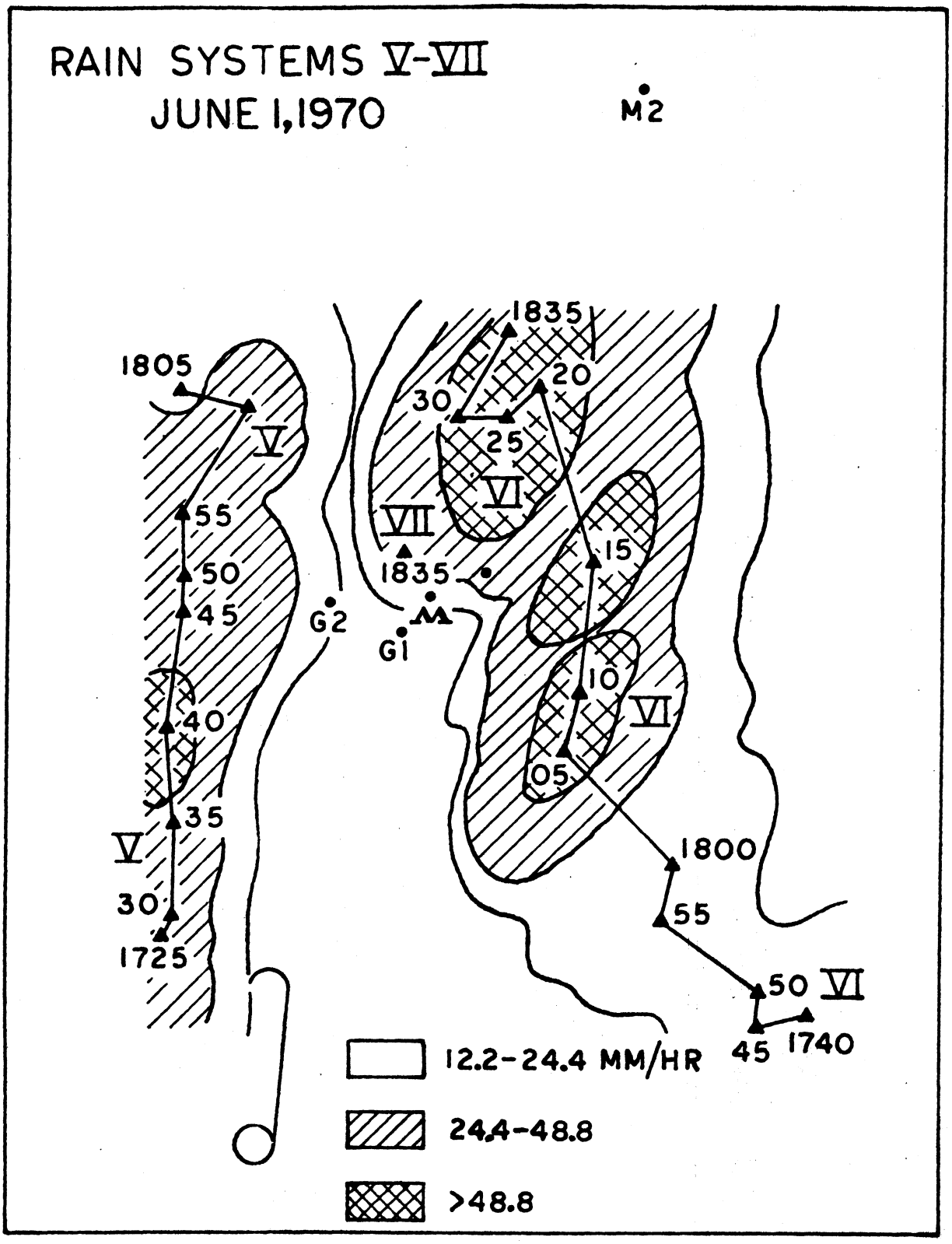

Figure 8b. Ten-minute isohyet envelopes for rain systems V through VII, 1720 to 1840 CDT

iii. Tracer plume transport estimation.

Although the experimental design and execution aimed to place tracer only in the major leading updrafts of the advancing weather system, the borders of these currents are not clearly evident, and the aircraft path of some 16 km is almost certain to have entered some downdrafts during the burn. Thus the transport and dispersion of tracer may have taken either of two principal directions, that consequent upon going upward above the "frontal surface" or downward through the "frontal surface". The previous discussion of the wind field indicates that the upward moving tracer should encounter northward moving air whereas the downward moving portion could penetrate to the southwestward currents in the lowest post-frontal air. Isochrones for the leading (t_i, t_i') and trailing (t_f, t_f') edges of the tracer plume, assuming direct advection by the mean wind, are indicated for each of these possible trajectories in Figure 9.

iv. Sequential sampling data.

Figure 10 displays the rainfall rates and tracer concentrations in the sequential samples of rain water collected at the six sequential sampling stations, as functions of time. Note that the stations G2, G1, M and G3 are quite close together. The distance from G2 to G3 is 7 km, and the range of distances from the tracer flare ignition point is 17 km (G1) to 21 km (G3).

The showers that appear in Figure 10 are now identifiable with the respective radar echoes and rain systems of Figures 2 and 8. First rain was received at station G2 in the period 1700-05,

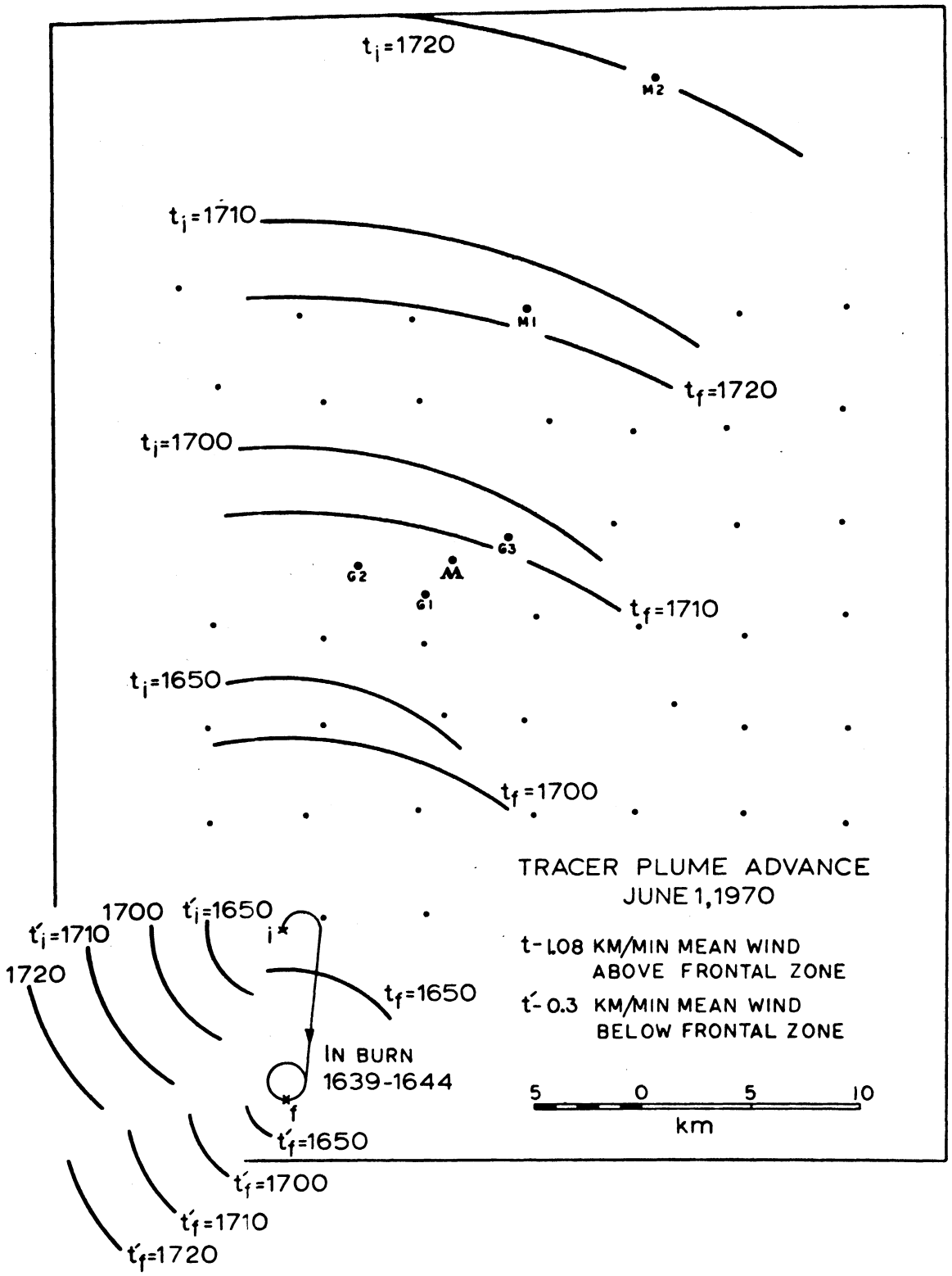

Figure 9. Estimated isochrones of tracer cloud, leading and trailing edges

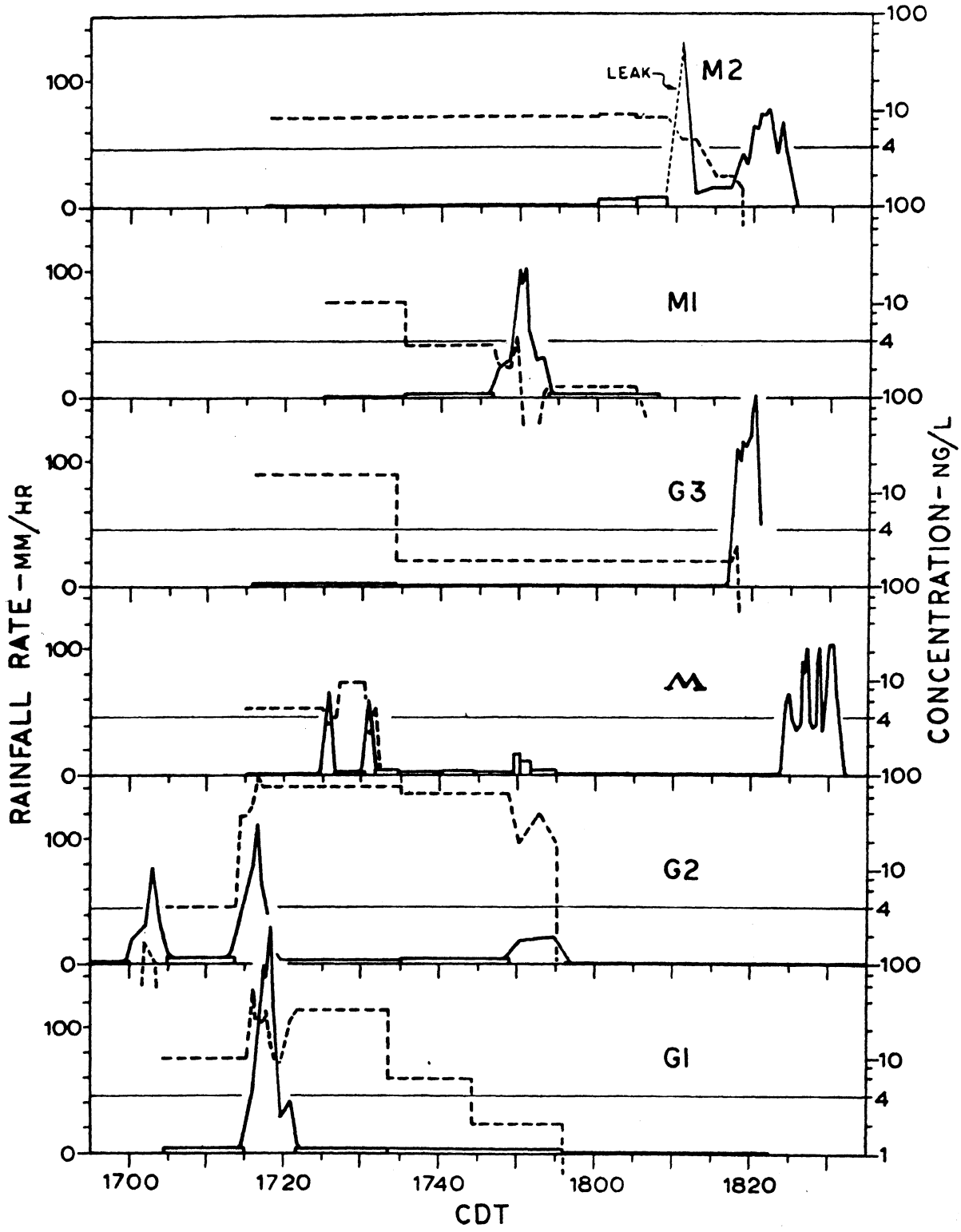

Figure 10. Temporal distributions of rainfall rate (solid lines, left ordinate) and In concentration (dashed lines, right ordinate) at the sequential sampling stations. Background concentration of 4 ng l^{-1} is indicated for each station.

and this is identified with radar echo track A (Figure 2a) and rain system I (Figure 8a). It is clear from all three figures (2a, 8a, 10) that this shower did not contain tracer indium. The light rain, 1705- 15, at stations G2 and G1, however, contained larger concentrations of In, exceeding the background level at G1, and just reaching it (4 ng l^{-1}) at G2 (Figure 10). Figures 2a,b indicate that this rain was

(a) at station G2, first composed of post shower spray containing no indium tracer, from radar track A, and later possibly contributed to by pre-shower spray, labeled by tracer, from radar track D (system I, Figure 8a)

(b) at station G1, a smaller amount of spray from track A, and a larger contribution from track D.

Hence both samples apparently contained tracer diluted by non-labeled rain water from the earlier shower, but more diluted at G2 than at G1.

With the onset of the shower 1715-25, the tracer concentration rose abruptly at G2 and G1, reaching its overall maximum value with the shower climax at G2 (Figure 10). That the concentration increased despite the diluting effect of the increasing rainfall rate indicates clearly the arrival of rain identified with the main tracer plume. This rain is also identified in Figure 2b with radar tracks D (station G2) and D_1 (station G1).

The initial spray and small shower at M , 1715-25, is also best identified with the same radar echoes, but evidently

with the eastern edge of the shower. Here the tracer concentrations are much lower, and in their variation with respect to rainfall rate, they follow the pattern of a well-mixed aerosol, namely, dilution with increased rainfall rate. The second small shower at M, 1730, is evidently identified with early rain from radar echo track D2 (Figure 2b). The small amount of tracer present in this shower suggests that the eastern edge of the tracer plume had been only minimally entrained by this shower at this time, and no tracer indium was found in the samples from station M after 1730.

Station G3 received only spray, probably from the radar track D1 shower, in the period 1720-'35, the sample for which contained definite tracer indium. This suggests that the outflow aloft from this shower extended strongly eastward across the general S to N winds shown by the soundings (Figure 4,5).

At station G2, following the 1715-20 shower, the tracer concentration persisted at a high level in light rain until 1750 when a small shower deposited the last of the tracer found at this station. The radar was shut down at 1745 so it did not show this event, but the rain system analysis (Figure 8a) indicates that it was associated with system V. The small shower at M at this same time, however, was probably a residual effect of the undesignated rain system south of system II in Figure 8a.

The isochrone projection of Figure 9 indicates a problem with the persistence of tracer at these four stations (G2, G1, M, G3) after 1710, but at the same time it justifies the appearance of the tracer at M1 and M2 by 1720, if the upper

level south-to-north air trajectory is assumed. If, however, a low level southwestward trajectory for some of the tracer is invoked, the tracer-labeling of system V (Figure 8b) is seen to be quite reasonable, and the timing of the tracer-labeled rain at G2 at 1750 is justified. Further, the westward spread of the tracer deposition pattern (Figure 6) is also consistent with low-level tracer transport into system V.

At stations M1 and M2, respectively 31 and 43 km from the initial tracer emission point, tracer is also identified in rain up to 30 to 40 min. after passage of the estimated t_f isochrone (Figure 9). The shower at M1, 1747-53 (Figure 10), may be identified with the projection of radar echo track D_2 (Figure 2b) and rain system III. The indium concentrations, though marginal, indicate that an unmixed remnant of the tracer plume entered this shower system because, within the shower, the concentration increased with rising rainfall intensity. The shower at M2, 1810, is most likely identifiable also with rain system III even though neither the radar nor the rain gauge data extend to this location. The persistence of tracer concentrations above background through this shower is an important indicator. The final shower system at M2, 1817-1825, evidently contained no tracer and served to complete the removal of residual tracer left by the previous system.

c. Interrelationships of tracer and rain data.

Certain features of the rain and tracer distributions brought out by this experiment can be generalized:

(1) Most of the observed tracer deposition pattern (Figure 6) was produced by a self-propagating system of showers

identifiable in the radar echo sequence (Figure 2a,b) as the series B, D, D1, D2.

(2) This sequence can be extended by inference based upon the raingauge data, upon timing, location, shower intensity and the presence of tracer, to D3 (system III) and, further, but somewhat more tentatively to D4 (system IV).

(3) Characteristics of the self-propagating series are:

a) the regular appearance of new echoes at intervals of about 20 min.,

b) the location of each new echo at 5 to 6 km SSE of its predecessor at the time of first sight of the new echo,

c) motion of echoes in the general direction of the warm air winds in the 700-500 mb layer with speeds varying from about 70 percent to about 120 percent of the mean wind speed in that layer,

d) association of low speed of echo motion with developmental stage and of high speed with decay stage

e) echo "lifetime" of 30-35 min.,

f) rainfall intensity maximum of each shower somewhat greater than 100 mm hr^{-1} with the exception of the initial shower (echo B: data from rainfall analysis indicates 10-min. mean intensity below 12.2 mm hr^{-1}).

(4) A considerable mass of tracer material was carried southwestward in the air flow beneath the "frontal surface" (Figure 3, 4), and was subsequently carried back onto the network in conjunction with rain system V and/or was deposited by dry processes along and beyond the western edge of the network.

D. DEPOSITION SUMMARY AND THE BUDGET OF TRACER INDIUM

The data of Figure 6 are reasonable and continuous enough to justify further analysis and interpretation.

1. Axial Decrease of Maximum Deposition

Figure 11 shows the pattern of deposition of tracer along the principal axis of maxima. The x-distance scale is shown at the left of Figure 6. Observed values are shown by circled points. Values along the straight line are designated $\hat{D}_x$, and are expressed by

$$\hat{D}_x = \hat{D}_o \exp(-C_1 X) \qquad (1)$$

where

$$\hat{D}_o = (2)^{11.2} = 2350 \text{ ng m}^{-2}$$

and

$$C_1 = .0624 \text{ km}^{-1},$$

i.e., $\hat{D}_x$ decreases by a factor of 2 in about 10 km.

To fit the observed points more closely, the pseudo-periodic fluctuation may be expressed by

$$D_x = D_o[\exp(0.2079 + 0.00866X)\cos\frac{2\pi X}{12.4} - C_1 X] \qquad (2)$$

which gives the points marked by X's in the figure. Whereas $\hat{D}_x$ may be interpreted to be indicative of a mean scavenging effect operating upon a diffusing cloud of tracer, tne non-uniformity of the diffusion processes and of the rainfall field is

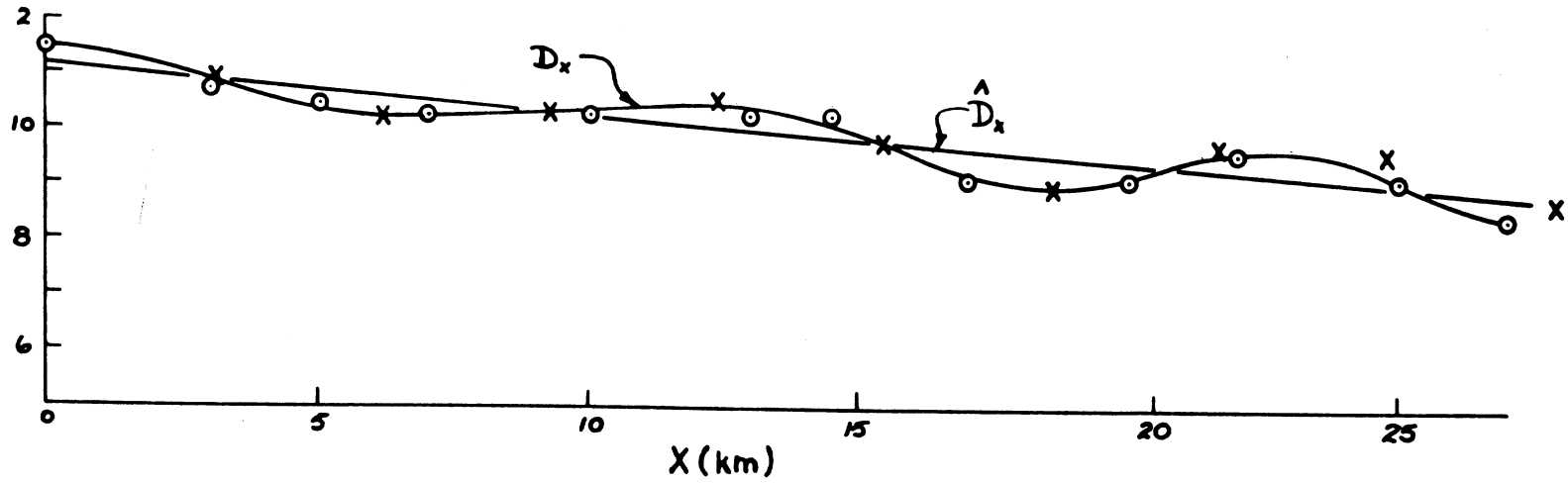

Figure 11. Tracer indium deposition along the principal axis of maximum deposition

expressed nominally by the periodic factor. The 12.4 km wave length appears to characterize the field only briefly, but corresponds well with a convective cycle of about 25 min in a translational field moving at about 0.5 km min^{-1}. The latter corresponds closely to the radar echo propagation speed. The relation of these figures to the dynamic properties of the convective system remains to be developed in connection with the dynamical model.

2. Axial Profile of Total Deposition

To estimate the total deposition, lateral profiles across the deposition pattern were constructed and integrated graphically to give the total deposition for each profile. The result of this integration is shown in Figure 12.

Three domains of deposition are apparent, and these may be expressed by

$$\text{(a)}\quad \frac{dM}{dX} = 15\exp(-.105X),\ 0 \leq X \leq 6 \text{ km}$$

$$\text{(b)}\quad \frac{dM}{dX} = \text{constant},\ 6 \leq X \leq 14.5 \text{ km} \qquad (3)$$

$$\text{(c)}\quad \frac{dM}{dX} = 17\exp(-.051X),\ 14.5 \leq X \leq 30 \text{ km}$$

where M is the total deposition in gm of tracer indium. We interpret these domains, respectively, as

(a) primarily dry deposition and washout of the largest tracer-bearing particles, ($r \geq \sim 5\mu m$);

(b) the tail of (a) plus the wet deposition of nucleating particles after the time delay required for ascent of nuclei ($r \geq \sim 1\mu m$) and growth of cloud droplets;

(c) entirely wet deposition, primarily by nucleation of tracer-

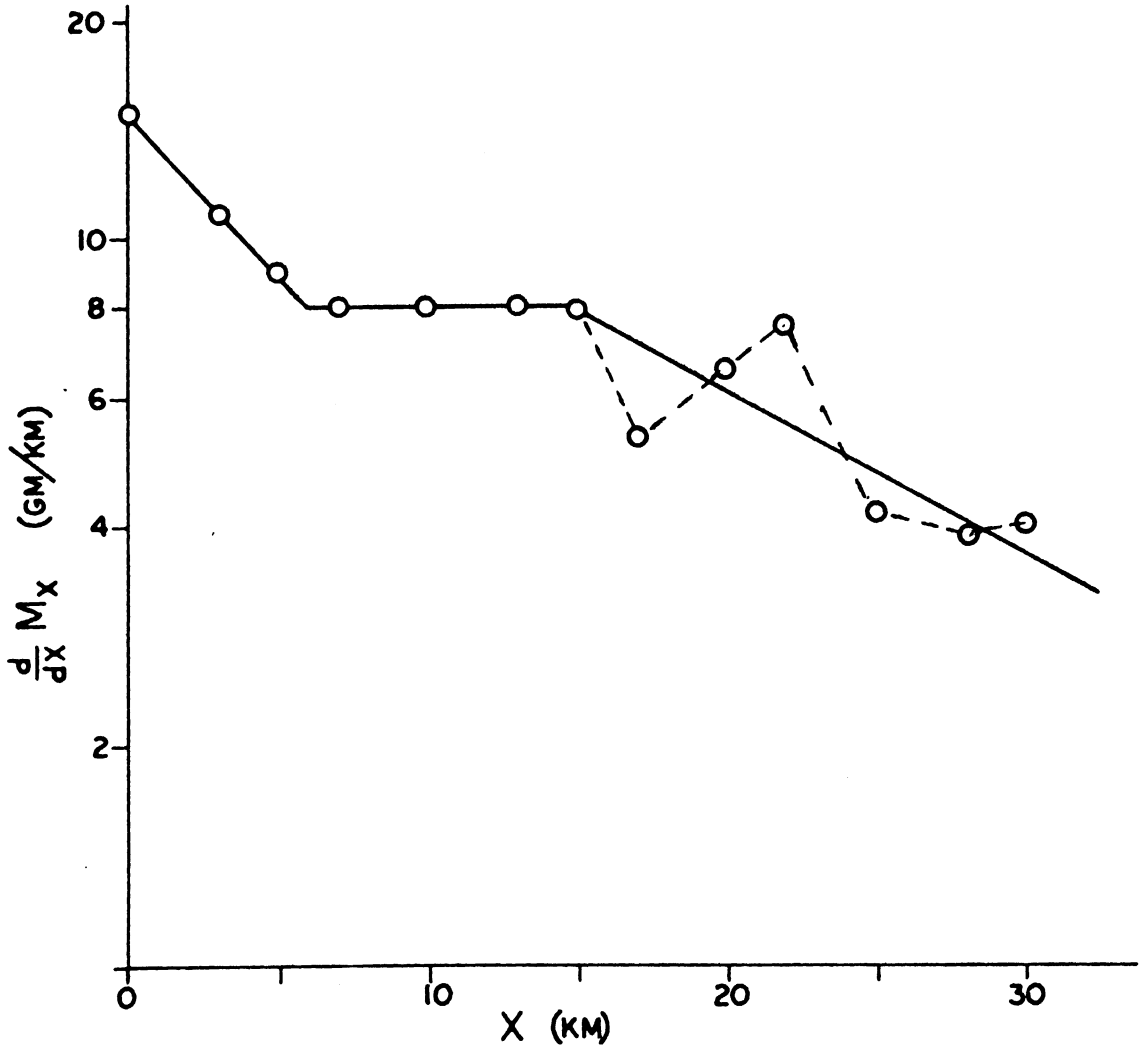

Figure 12. Longitudinal profile of laterally integrated deposition amounts

bearing particles, but with a contribution due to diffusive attachment that increases with distance downstream in relation to the contribution of the nucleation process ($0.2\mu m \leq r \leq .2\mu m$ plus $r \leq .03\mu m$)

3. Integration and Adjustment

Integration under the profile of total deposition to the 30 km distance (as indicated at the left of Figure 6) gives a deposition total

$$M_{0-30} = 226 \text{ gm.}$$

The total emission of indium tracer was 543 gm, hence this initial summation accounts for 42 per cent of the emitted amount.

It is clear from Figure 6 that the deposition pattern continues considerably beyond 30 km. Station M2 is 43 km from the point of ignition of the flares. The westward and southward spread of the deposition is also evident in Figure 6 and has been discussed above. We propose here to estimate the amounts of tracer indium associated with these extensions of the deposition pattern:

(a) Assuming an extension of domain (3c) to 100 km, additional deposition of 70 gm of indium is computed; extending to an infinite distance, the still further increment is only 2 gm.

(b) Extrapolating the lateral profiles westward to a baseline of 32 ng m^{-2}, the westward drift off of the network is estimated at 14 gm.

(c) Assuming that the actual deposition maximum lies 2 km south of the network, and integrating (3a) to this distance gives 33 gm additional.

(d) Finally it is assumed that 12 gm more of indium tracer was deposited south of the deposition maximum.

Combining these estimates with the network total gives 355 gm or 65 percent of the total tracer emission.

4. The Residual Tracer Material

To account for the 35 percent residual of tracer material, a certain amount of reasoned speculation is necessary. Basically we know that 65 percent is a relatively high, but reasonable, figure for the efficiency with which a moderate convective storm converts water vapor to rain (Gatz, 1966; Newton and Fankhauser, 1964). It is not unreasonable that it should scavenge the tracer material (or other component of mixed nuclei) with a similar efficiency. The residual of water is recognized to reside in residual cloud droplets which eventually reevaporate and in uncondensed vapor; the residual of tracer may analogously be presumed to reside in the residual cloud droplets as attached or dissolved material and in the cloud air as unattached particles. It may further be inferred that the bulk of the cloud-droplet - attached tracer must be there by virtue of the nucleation of liquid water upon the original tracer-bearing particles, but that these nuclei were originally relatively small. The residual of tracer material is thus mainly identified with the size range $r < 0.4\mu m$ or so. That in the range $r < 0.03\mu m$ may be considered sufficiently dynamic to have attached to cloud droplets by diffusive processes over the cloud lifetime. The portion in the range $r > 0.2\mu m$ or so are presumed to serve as condensation nuclei. The portion in the

range $0.03 \leq r \leq 0.2\mu m$ are thus estimated to remain in the cloud air as inferior nuclei and relatively non-dynamic particles under the diffusive forces; these represent 12 to 15 percent of the total tracer mass.

E. CIRCULATION, SCAVENGING, AND MODELLING CRITERIA

The observations, measurements, and inferences presented above offer a detailed description of the self-propagating convective system in its relation to other rain-producing portions of a typical midwestern summer squall line. The features of this system should evolve from an adequate numerical model of the squall line. That such a model is relatively remote from realization at the present time must also be noted. Nonetheless, the direction of fruitful convective system modelling effort is indicated, and several basic criteria for a "satisfactory model" are contained in this case study.

1. Circulation

The circulatory characteristics of convective storms have been explored and described in many publications. These will not be reviewed in detail here. The broad features of the most intense types appear to be best described by Browning and Ludlam (1962), by Newton (1967), by Fujita and Grandoso (1968), and by Fankhauser (1969). Generally the focus of these descriptions is upon the wet phase of the convection. Fankhauser suggests that the convection might disturb an area twice the diameter of the typical radar echoes.

It is therefore well-understood that a convective storm is fed from below by a major updraft which supplies cloud condensation nuclei and water vapor copiously. The horizontal convergence below and divergence aloft are understood conceptually, but circulatory details of these processes are not well-described. Rather, the outflow aloft, labeled by the great anvil streamer, is recognized universally as an obvious feature, whereas the spacing of active storm centers, the return flow regions, and the broad scale dry-process subsidence and divergence patterns of the storm environment are not adequately resolved by previous studies. Yet it is clear that no storm model neglecting or omitting these environmental processes can adequately simulate the circulatory features of convective storms.

The self-propagating sequence of showers is an outstanding feature of the present experiment. In terms of "storm" and "relevant environment" regions, we have from these data that

(a) whereas the updraft region of a "storm" of this series has a radius of about 2 km, the distance to the next generation "storm" at the time of its first radar echo is 5 to 6 km;

(b) the regions of convergence below and of divergence aloft necessarily extend much farther, to perhaps 30 km or so, but not symmetrically, i.e., the anvil plumes show divergence extending in the downwind direction in the 6-9 km layer, whereas the new echo development indicates a maximum of convergence in the 0-3 km layer roughly 90 deg to the right of the anvil plume;

(c) the lifetime of each continuously identifiable radar echo (rain mass) is 30 to 35 min.; it is reasonable to assume that updraft and cloud initiation precede first radar echo by about 15 min and that diffuse spray-type fallout of stored water continues for 10 min or so after the radar echo has faded into the background, thus total shower lifetime is about an hour;

(d) the 20-min period between successive generations of the shower sequence is remarkably constant.

The penetration of tracer material through the squall front and southwesterly off the edge of the network, to a distance of the order of 10 km, indicates a circulational feature which has not previously been emphasized. This feature is consistent with downdraft effects upon the tracer plume up to, but probably not more than, about one-third of its length. Figures 13a,b show the shape and extent of radar echoes for the period 1639-1745 CDT. Inasmuch as echo A was not labeled by the tracer, it may be inferred that the northern end of the tracer plume was not coincident with the updraft feeding that echo. It is entirely consistent with the radar echo pattern and the rainfall pattern to recognize the presence of downdraft regions among the updrafts along the tracer burn path.

2. Scavenging

The three basic rain scavenging mechanisms of nucleation, diffusion, and impact collection are probably augmented by dry deposition to some unknown extent in the present

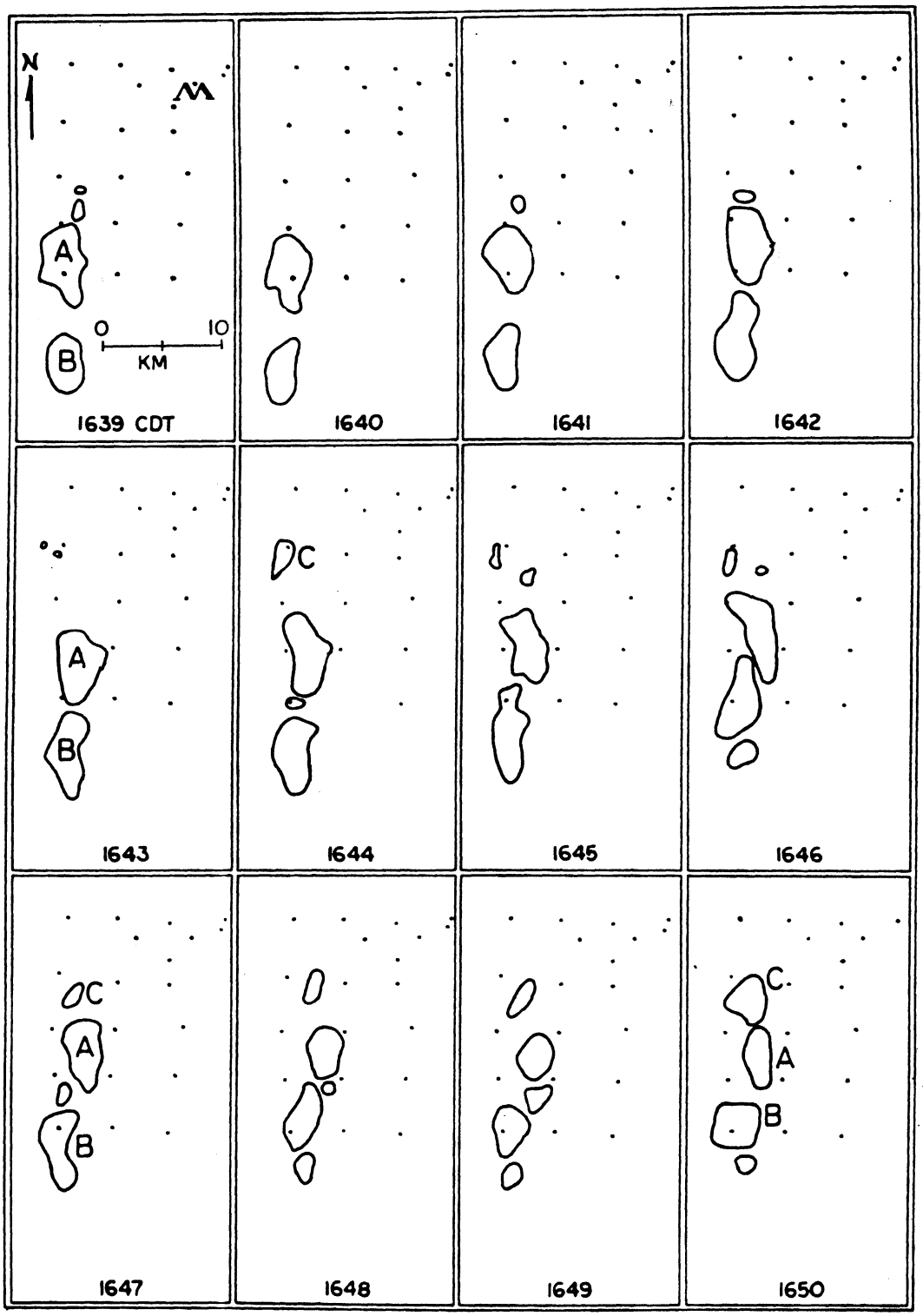

Figure 13a. Radar echo patterns 1639-1650 CDT

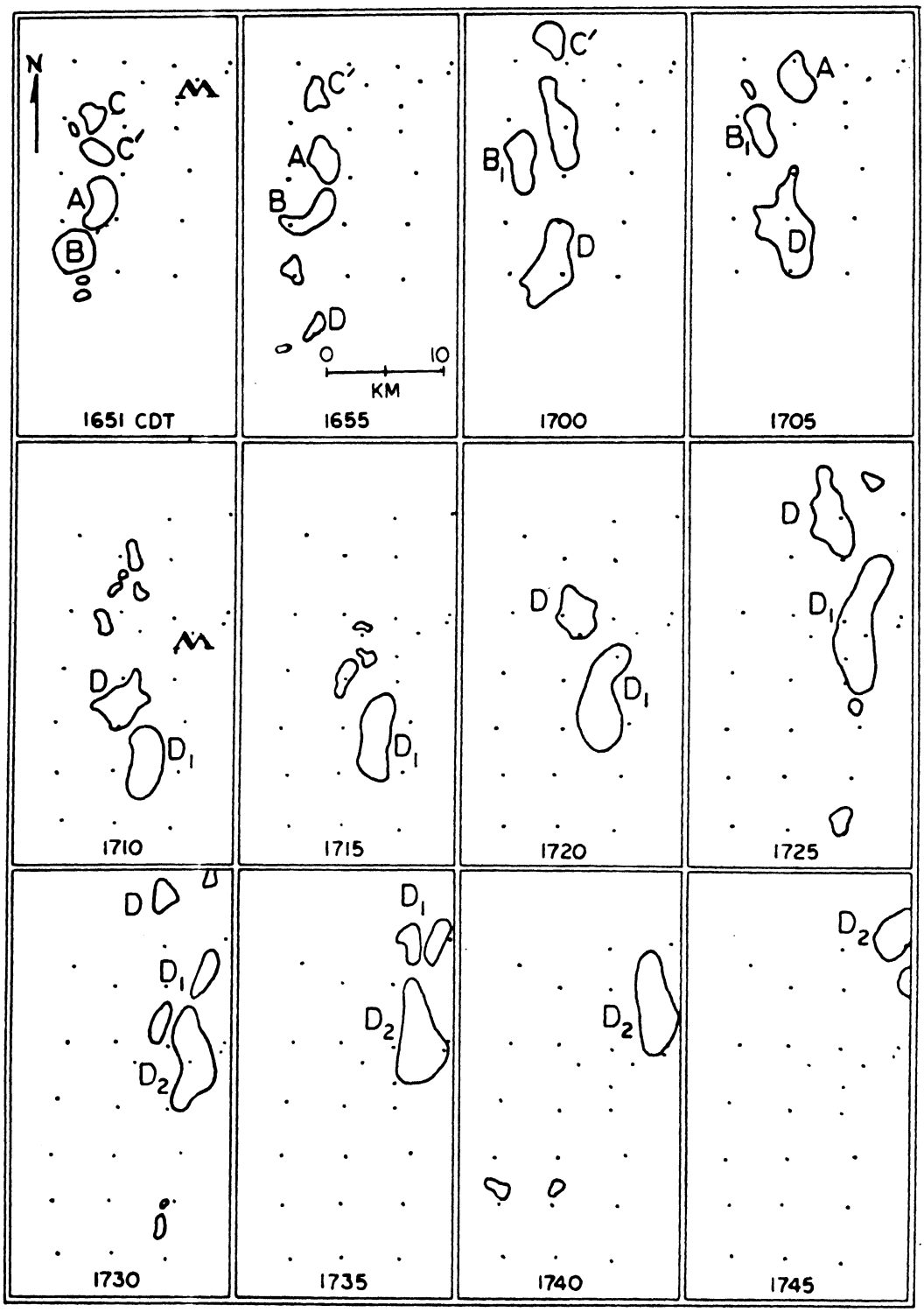

Figure 13b. Radar echo patterns 1651-1745 CDT

data. Although the best information on particle sizes of the flare plume indicates a very small number of particles larger than 1μm in radius, photographic evidence of the flare performance in flight (Figure 14) indicates that relatively large pieces of the flare material tend to be ejected, and these could carry large amounts of tracer to earth directly. The tracer deposition pattern indicates that this process probably contributed to the principal maximum, particularly in view of the rainfall minimum in this area (Figure 7).

The extension westward of the deposition pattern might also have a dry deposition component because low level dry transport of the tracer is the only conceivable mechanism, within the context of the observational data, that could have carried the tracer so far south and west. The magnitude of this component of the deposition is unknown. The rainfall along the western limit of the network, particularly from rain system V (Figure 8b) is sufficient and is well-timed to have made the major contribution to this part of the pattern.

Aside from the unknown contribution of dry deposition, the entire deposition pattern can be adequately explained in terms of the model of Dingle and Gatz (1966), i.e., the present data support most logically a low level input mechanism to each tracer-depositing shower. Particularly is this indicated by the sequential sampling data (Figure 10), where it can be seen that both pre-shower spray and post-shower residual rain tend to contain moderate to high concentrations of tracer, but shower

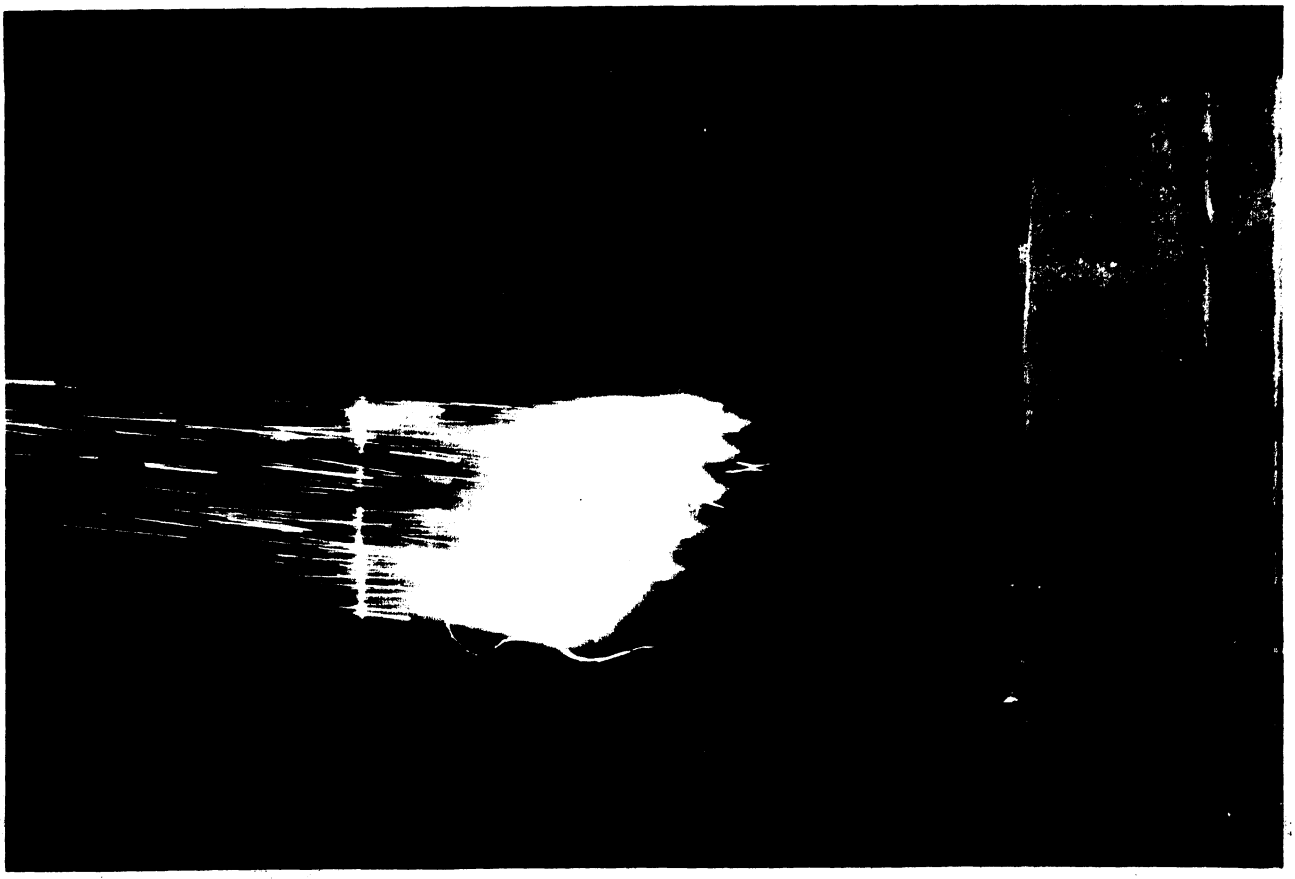

Figure 14. Indium flares burning in flight. Large particles are indicated by bright lines.

onset is frequently accompanied by an upward pulse of the concentration in the tracer-bearing showers. It remains difficult dynamically and geometrically to support the idea of tracer input from the top of the active showers. Further, there is no need for input to these showers but from below. The high concentrations in the light rain portions are readily explained in terms of evaporation over a long sub-cloud fall path, and a minor contribution of impact collection over the same path. The upward impulse of concentration with rising rainfall rate can only be attributed to a strong relative increase of tracer associated with the condensation nuclei fed into the system by its principal updraft.

3. Modelling

Although one- and two-dimensional models of convective processes have contributed insights into some aspects of the problem, the growth and decay patterns and the asymmetries evident in most natural convective systems indicate that they must be studied as time-variable systems in three dimensions. Further, to comprehend the wet and the dry components of the system, circulatory features out to 6 or 8 times the radius of the central rain-producing region are required, and the boundary conditions even at such distances may be quite variable. The self-propagating series of showers observed in the present case study gives evidence of a periodicity that may prove helpful in solving the modelling problem, however this characteristic also

emphasizes the need to include the storm environment far from the original convective cloud. The showers that respectively preceded and followed the self-propagating series at the western edge of the network were, on the other hand, aperiodic, implying a time-variant effect of the environment. This effect may be seen in a well-designed model, but is probably not central to the early phases of the modeling effort.

Grid spacing smaller than about 0.5 km appears to be required. In the vertical direction, the grid should probably not exceed 0.2 km, whereas 0.5 km may be sufficiently fine for the horizontal directions. If such a grid can be used, a cubic computational domain of 16 grid spaces in each direction may suffice to model a circulatory system simulating the basic elements of the present case study.

In approaching the question of wet-process simulation, it is doubtful whether the above grid is of sufficiently fine mesh. Although a practical model must eventually incorporate the wet processes by means of parameterization, it appears clear at this juncture that the parameterization procedure used most frequently (Kessler, 1969) is not adequate for the present purposes. In short, improved parameterization is required, and full scale computational treatment in a very fine grid appears to be required to develop and test a suitable parametric scheme.

F. REFERENCES

1) Bhatki, K.S., and A.N. Dingle, 1970: The measurement of tracer indium in rain samples. J. Applied Meteor. 9, 276-282.

2) Browning, K.A., and F.H. Ludlam, 1962: Airflow in convective storms. Quart. J. Roy. Met. Soc., 88, 117-135.

3) Dingle, A.N., 1970: Scavenging of tracer in severe storms. In Precipitation Scavenging, AEC Symposium Series 22, pp. 21-35.

4) Dingle, A.N., and D.F. Gatz, 1966: Air cleansing by convective rains. J. Appl. Meteor. 5, 160-168.

5) Dingle, A.N., D.F. Gatz and J.W. Winchester, 1969: A pilot experiment using indium as tracer in a convective storm. J. Appl. Meteor. 8, 236-240.

6) Engelmann, R.J., 1968: The calculation of precipitation scavenging. In Meteorology and Atomic Energy, 1968, D.H. Slade, ed. U.S.A.E.C. Technical Information Division, TID-24190, Clearinghouse, p. 209.

7) Fankhauser, J.C., 1969: Convective processes resolved by a meso-scale rawinsonde network. J. Appl. Meteor. 8, 778-798.

8) Fletcher, N.H., 1962: The Physics of Rain Clouds. London, Cambridge University Press, 386 pp.

9) Fujita, T., and H. Grandoso, 1968: Split of a thunderstorm into anticyclonic and cyclonic storms and their motion as determined from numerical model experiments. J. Atmos. Sci. 25, 416-439.

10) Gatz, D.F., 1966: Deposition of atmospheric particulate matter by convective storms: the role of the convective updraft as an input mechanism. Ph.D. dissertation, Department of Meteorology and Oceanography, The University of Michigan, Ann Arbor, 216 pp.

11) Gatz, D.F., R.F. Selman, R.K. Langs, and R.B. Holzman, 1971: An automatic sequential rain sampler. J. Applied Meteor. 10, 341-344.

12) Greenfield, S.M., 1957: Rain scavenging of radioactive particulate matter from the atmosphere. J. Meteor. 14, 115-125.

13) Junge, C.E., 1963: Atmospheric Chemistry and Radioactivity. New York, Academic Press, 382 pp.

14) Kessler, E., 1969: On the distribution and continuity of water substance in atmospheric circulations. Meteor. Monographs 10, no. 32, Amer. Meteor. Soc., 84 pp.

15) Newton, C.W., 1967: Severe convective storms. Advances in Geophysics, Vol. 12, pp. 257-308.

16) Newton, C.W., and J.C. Fankhauser, 1964: On the movements of convective storms, with emphasis on size discrimination in relation to water budget requirements. J. Appl. Meteor. 3, 651-668.

II. Modelling of Cloud Microphysics

A. Introduction

In approaching the general problem of modeling the scavenging functions of convective shower systems, the problem of the wet microphysical processes obviously arises and needs to be treated in this particular context. Whereas several prior convective models have treated the wet processes by means of Kessler's parameterization scheme, and this approach appears to give plausible results in some cases, it is generally agreed that the wet processes require a physically more realistic treatment (e.g., Ogura, 1974). This fact is emphasized in the scavenging problem which doubly depends upon microphysical processes.

It is also clear, however, that parameterization of the microphysics must be used in any practical operational convective system model. The form of parameterization that will at once fulfill the requirements of physical fidelity and of computational feasibility remains to be developed.

B. Equilibrium vs Non-Equilibrium

Mason (1957), by a series of ingenious maneuvers, devised the generally accepted derivation of "the droplet growth equation":

$$r \frac{dr}{dt} = \frac{(S - 1)}{(L^2 M\rho / KRT^2) + (\rho RT / p_s(T) DM)} \qquad (1)$$

The major assumption underlying this equation is that the vapor transfer and heat transfer processes are exactly in equilibrium for the growing droplet at all times, i.e., that latent heat is transferred to the droplet environment at exactly the rate that it is released by the condensing vapor.

Considering that the thermal relaxation times for cloud droplets lie in the range of 10^{-5} to 10^{-3} sec, the equilibrium assumption appears to be quite sound. The problems it raises pertain less to its physical reasonability than to the numerical instabilities that arise at the small-size end of the droplet spectrum. To maintain computational stability using (1), Fitzgerald (1972) has shown that the time step must be limited to 10^{-2} sec for droplets formed on 10^{-17} gm NaCl nuclei. Arnason and Brown (1971) show that the limiting time step decreases for smaller droplets and/or larger number densities. More recently, however, Brown and Arnason (1973) have adapted an implicit numerical scheme (Liniger and Willoughby, 1970) which enables the relaxation of this requirement.

Storebo and Dingle (1974), on the other hand, have devised a procedure in which the vapor-to-liquid phase change and the transfer of released latent heat are computed sequentially and linked through a feed back mechanism in each time step. In this scheme, the vapor and heat transfer rates determine the end state without requiring that equilibrium be achieved. Although the relative fidelity of this approach and the imposed equilibrium

approach may be argued, it is found that the computations remain stable for time steps of the order of seconds in the Storebo-Dingle scheme.

This problem is under study. After nucleation, each growing droplet follows a course of growth given by the unstable segment of its Kohler curve. For the equilibrium equation, as long as exact equilibrium is maintained, the computation is all right, but very minor numerical departures from equilibrium have the effect of introducing large perturbations in response to the physical instabilities these departures represent. In the case of the smallest droplets, which have large number densities, the effect upon the water budget of the cloud becomes excessive. Sufficient perturbation can result from round off errors in the smallest size classes. For the non-equilibrium computation, on the other hand, the equilibrium condition is approached, but seldom if ever actually achieved. The effect of round off error is thereby controlled within reasonable bounds, enabling relatively large time steps even for the small-size droplets of high number density.

A numerical exercise, RADFOG, for cloud physics students, affords some insight. The exercise is designed to simulate the development of a radiation fog in the absence of sedimentation and advection. A constant rate of radiative cooling is assumed for air of specified humidity containing a specified size spectrum of airborne nuclei the chemical properties of which are also specified. The latent heat released as the fog forms and grows

simply moderates the cooling effect. The computations are carried through nucleation and growth over an extended time period. After an hour or so the droplet size spectrum becomes very narrow, but each of the size classes retains its own integrity. The humidity lowers steadily toward 1, but the equilibrium humidity for the smallest size class remains very slightly higher than that for the larger ones. Eventually, the humidity falls below that required to maintain the smallest droplet-size class, which thereupon evaporates abruptly back to its pre-nucleation equilibrium point. The consequent abrupt release of a relatively large mass of water then contributes to rapid growth of the remaining drops. Although the absence of sedimentation makes this experiment valid only for a zero-gravity situation, the destabilizing effect upon a droplet population of the approach to vapor equilibrium is clearly shown.

A comparative computation using the scheme of Brown and Arnason (1973) is planned, and a theoretical analysis of the two approaches is in preparation.

C. The Parameterization Problem

Convective models incorporating the wet processes have most generally adapted the parameterization proposed by Kessler (1969). In this scheme all vapor excess over 100 per cent relative humidity is converted to rain, and any saturation deficit is restored by evaporation as long as liquid water is available. As a first approximation, these provisions are probably acceptable, but in the event that more detail and/or better fidelity of simulation is required, this parameterization scheme is inadequate.

At the present juncture it appears that a satisfactory parameterization scheme for the microphysics must be proven by comparison against the more complete microphysical computations for similar cases. There are additional considerations which are not wholly resolved. For example, Miller and Pearce (1974) find that the cloud dynamics is "...quite sensitive to assumptions made regarding the cloud microphysics...". In turn, Storebo and Dingle (1974) have found that the microphysics may be "quite sensitive" to rather small scale dynamic features within the clouds. The possibility arises, therefore, that the parameterization sought may be required to resolve scale problems in both the dynamics and the microphysics. Our current approach to the question is two-pronged. The one approach begins with the microphysics and seeks to define those scales and frequencies of dynamic features that interact most strongly with droplet growth and evaporation cycles. The other approach is from the dynamics side, and seeks to define the small-scale dynamic features in relation to the larger ones. One fact is clear: we require the most advanced and sophisticated modeling techniques to do an adequate job of convective system modeling for the purpose of predicting rain scavenging and deposition patterns. These will probably be subject to eventual simplification via parameterization, but the most appropriate forms of parameterization still need a great deal of theoretical study and applicational testing.

D. References

1) Arnason, G., and P.S. Brown, Jr., 1971: Growth of cloud droplets by condensation: a problem in computational stability. J. Atmos. Sci., 28, 72-77.

2) Brown, Jr., P.S., and G. Arnason, 1973: Efficient numerical integration of the equations governing droplet growth by condensation. J. Atmos. Sci., 30, 245-248.

3) Fitzgerald, James W., 1972: A study of the initial phase of cloud droplet growth by condensation: comparison between theory and observation. Ph.D. dissertation, Department of Geophysical Sciences, The University of Chicago, 144 pp.

4) Kessler, E., 1969: On the distribution and continuity of water substance in atmospheric circulations. Meteor. Monographs 10, no. 32, Amer. Meteor. Soc., 84 pp.

5) Mason, B.J., 1957: The Physics of Clouds, London, Oxford University Press, 481 pp.

6) Miller, M.J., and R.P. Pearce, 1974: A three-dimensional primitive equation model of cumulonimbus convection. Quart. J. Roy. Meteor. Soc., 100, 133-154.

7) Ogura, Y., 1974: Personal letter of 28 June 1974.

8) Storebo, P.B., and A.N. Dingle, 1974: Removal of pollution by rain in a shallow air flow. J. Atmos. Sci., 31, 533-542.

III. Remarks to DNA Rainout/Washout Conference, 4-5 June 1974; Defense Nuclear Agency Hq., Alexandria, Va.

Inasmuch as I am a newcomer to this series of conferences, and I am a meteorologist who has engaged in studies of the relevant phenomena at all the scales from nucleus formation and cloud microphysics to convective storm dynamics to synoptic scale analysis and prediction, both in terms of field experiments and numerical modeling, it may be appropriate for me to provide some general perspectives on the systems we are dealing with, and thus to aid in defining the environment within which we are working and some of the specific problems that should have a relatively high priority.

A. Precipitation and precipitating weather systems.

Although these have great variability, let us give attention first to the common characteristics:

1. By and large the important precipitation is produced in air that is forced upward by some mechanism. In the course of upward motion, cooling takes place and excess water vapor condenses upon airborne nuclei. The nuclei and the water vapor are necessarily mixed together in the upward moving air. The sole water vapor source is the Earth's surface, hence low level mixing is a prerequisite.

2. The uplift of air generally requires a horizontally convergent flow at low level, which produces the upward displacement and contributes nearly all of the constituents for precipitation. This low level convergence is necessarily compensated by a horizontal divergence from the upper part of the updraft region.

3. The upward current is also necessarily compensated by downward flow in the environment of the updraft. The areal extent of downdraft is some tens of times that of updrafts.

   a. Satellite photographs show that clouds cover 40% to 55% of Earth's surface most of the time.

   b. Rainfall studies show that somewhat less than 10% of the cloud-covered area receives precipitation at any time.

   c. The residual 90% + of the cloud field area is mainly in divergent flow with a net downward drift, and this cloud material is in an evaporating stage.

B. Entrance of contaminant placed at high levels.

1. Small particle contaminant which originates at high level cannot enter efficiently or in large amounts directly to the rain-forming region of a cloud.

a. The top of the cloud is defined by updraft currents capable of supporting cloud droplets the fall speeds of which far exceed those of the submicron debris particles.

b. The upper lateral boundaries of the cloud are characterized by horizontal divergence and evaporation associated with slow downward motion.

2. Debris particles large enough to fall into the cloud against the cloud-supporting upward motions are actually slowed by these motions, but also are of such size as to be better and more simply considered in the category of close-in dry fallout.

3. The broad down-flow regions provide the means for small debris particles to be transferred systematically to low levels. This transport augments the gravitational sedimentation of the particles and initiates mixing with air detrained from the cloud field. As the cloud water evaporates in this process, the original cloud nuclei are released back to the air augmented in size by the material attached during the cloud droplet lifetime.

4. Mixing of the high level contaminant with low level aerosol and water vapor finally can proceed efficiently in the low "mixed layer" over a period

of hours to days. In this process, the original debris size-distribution loses its identity as, by attachment, it becomes indistinguishable from the boundary layer aerosol, except only for its radioactive properties and its chemical makeup.

5. At this point, the debris-containing tropospheric mixed aerosol is ready to enter a lifting process, to function as cloud condensation nuclei in and below a rain-producing region, and to be relatively efficiently removed and deposited upon the ground with rain. Available estimates of this efficiency vary from 45% to 65% based upon water budget studies. There is good reason to apply the same figures to the respective aerosol constituents.

C. Contaminant placed at low levels.

1. Define "low levels" to be within the field of horizontal convergence that contributes to updraft flow. This is mainly below about 3 km.
2. Define dry fallout to be those particles capable of sedimentation before reaching the updraft region, or of falling out against the updraft.
3. All remaining debris may be treated as
   a. Cloud droplet nuclei ($r \geq 0.2\mu m$)
   b. Airborne particles capable of in-cloud attachment ($r \leq \sim .03\mu m$)
   c. Greenfield gap particles ($.03\mu m < r < 0.2\mu m$)

4. Removal by rain will follow closely according to the efficiencies cited above applied to the total mass of contaminant (including the Greenfield gap). Note: although we do not have an effective defined mechanism to remove the "gap" particles, it is evident that they do not accumulate, hence they are removed: we do not yet know how in microphysical detail.

D. Modeling

1. The above descriptive model of the rain scavenging process is somewhat indicative of the scope required of any numerical simulation experiment designed to represent rain scavenging.

   a. It suggests that a great deal goes on outside the clouds in the way of preparation for the final process. In fact, it is probably true that an adequate model for this simulation should extend about ten storm diameters in each horizontal dimension. Unfortunately, atmospheric observations are not very complete in these areas, but Arakawa et. assoc. have suggested that in the tropics, at least, the downward displacement of dry "superior" air which is forced by convective cloud buildup represents the <u>principal</u> mechanism by which convective cloud actually heats the air at low levels.

b. Further, it is probably true that if the problem of modeling rain scavenging by convective systems can be properly solved, we should have in hand good solutions to the gamut of the rain scavenging problem.

2. Convective storm modeling is coming on rapidly. A number of the people here have been working productively in this area. Nonetheless, I should like to offer the following comments:

   a. It is readily feasible to construct idealized models of pseudo-convective systems in two dimensions including temporal dependency, BUT

   b. By and large these efforts fall short for one or more of the following reasons:

      1. parameterization so de-limits the performance of the model that it can at best reproduce only very limited aspects of the physical system, and this performance is dictated by the selected parametric values;

      2. cylindrical symmetry, which is very tempting as a model of convection, and which is nicely productive of realistic updraft simulation, cannot invoke a suitably shearing environment, and so fails on this account, as well as its overly symmetric form and excessively upright posture;

3. slab symmetric models can be sheared, but they lack the implicit 3rd-dimensional convergence which the cylindrical models have and so they give poor simulation of the updraft;
4. the interactions of the three components of the real motion field cannot occur in any of the two-dimensional models, and hence their simulative power is seriously impaired.

C. It is therefore essential that three-dimensional time dependent models be brought to bear upon the problems we face. The work of Deardorff, Lilly, Fox, of Murray, Ogura, Takeda, and many others has laid the groundwork upon which to proceed.

IV. Numerical Models for Precipitation Scavenging: Abstract

Two models are developed. The first is designed for precipitation scavenging in stratiform clouds. This model incorporates heuristic approximations of diffusive attachment, impact collection and accretion, and includes consideration of particle and cloud droplet size spectra. An overriding, independently generated steady rain removes contaminated cloud droplets and contaminant particles. The conservation of contaminant mass is expressed by a set of three ordinary differential equations for which analytic solutions are derived. Rainout ratios and efficiencies are computed, and the results compare favorably with available field measurements. It is shown 1) that no single attachment rate constant or removal rate constant can adequately express the removal by rain of airborne contaminant, 2) that the contaminant concentration in the cloud air decreases exponentially with time when the processes of diffusive attachment and rainfall removal are considered, and 3) that the fraction of the air concentration of contaminant that is attached to the cloud droplets is affected by processes of particle attachment and rainfall removal, hence its temporal change shows an initial rapid rise to a maximum which is followed by a variable decrease that depends upon the rainfall rate and the cloud water content.

The second model addresses the problem of air cleansing by a convective rain-generating system. Microphysical

processes such as Brownian motion and impact collection can be neglected because the residence time in the cloud of the particles is too short for Brownian attachment, and the particles are too small for efficient impact collection by raindrops. Therefore, in this model, raindrop growth and motion in spatial contaminant concentration gradients are of major concern. Numerical solutions for raindrops growing by coalescence with cloud droplets and moving in a cylindrically symmetric motion field within a steady-state cloud are provided. The drop breakup process is formally accounted for, and, in the sub-cloud region, evaporation is considered. The cloud water and contaminant concentration are assumed to vary both with height and horizontal distance from the updraft core. A bell-shaped updraft profile is assumed. The contaminant concentrations of individual raindrops are computed. Because the updraft core is identified with the maxima of liquid water content and contaminant concentrations, (a) the coalescence growth process is most rapid in the upward passage of droplets through the cloud rather than the downward passage; (b) high concentration of contaminant tends to be associated with the larger drops formed near the core and lower concentration tends to be found in the smaller drops formed farther away from the core, and these associations produce a positive correlation between rainfall rate and contaminant concentration. Sub-cloud evaporation, on the other hand, tends to produce a negative correlation between these two parameters because it affects the small drops much more strongly than the

large ones. Drops of different sizes can therefore have the same concentration, and under the assumed conditions a particular drop-size is identified with the minimum concentration.

Inasmuch as these several relationships are observed in field experiments, the present model fulfills the special constraints imposed by the field data at the same time that it represents a plausible combination of the characteristics of previous convective storm models.

V. Administration

A. Publications

C00-1407-45 "Removal of pollution by rain in a shallow air flow" by P.B. Storebo and A.N. Dingle. J. Atmos. Sci. 31, 2, 533-542, March 1974

C00-1407-46 "An analysis of in-cloud scavenging" by A.N. Dingle and Y. Lee. J. Applied Meteor. 12, 8, 1295-1302, December 1973.

C00-1407-47 "Ammonium sulfate crystallization in Andersen cascade impactor samples" by A.N. Dingle and B.M. Joshi. Atmos. Environment, 8, in press, July 1974

C00-1407-49 Rain Scavenging Studies by A.N. Dingle, Progress Report No. 9, Contract No. AT(11-1)1407, U.S. Atomic Energy Commission, Dept. of Atmospheric and Oceanic Sciences, The University of Michigan, Ann Arbor. July 1973. 116 + x pp.

C00-1407-50 Abstract of "A modelling study of droplet growth and rain scavenging in a convective system" by A.N. Dingle and Y. Lee. Conference on Cloud Physics, October 21-24, 1974, Tucson, Arizona.

C00-1407-51 Abstract of "Lanthanum-140 as a flux monitor in rain scavenging studies involving indium tracer" by K.S. Bhatki, A.T. Rane and A.N. Dingle. Conference on Nuclear Methods in Environmental Research, July 29-31, 1974, Columbia, Missouri

C00-1407-52 "Numerical models for precipitation scavenging" by Y. Lee. Ph.D. Dissertation, Dept. of Atmospheric and Oceanic Science, The University of Michigan, Ann Arbor. Also Scientific Report No. 2, Contract No. AT(11-1)1407, April 1974. 89 + x pp.

C00-1407-53 "A modelling study of droplet growth and rain scavenging in a convective system" by A.N. Dingle and Y. Lee. Preprint Volume, Conference on Cloud Physics, October 21-24, 1974, Tucson, Arizona, in press.

C00-1407-54 Abstract of "Scavenging and dispersal of tracer by a self-propagating convective shower system" by A.N. Dingle Precipitation Scavenging Symposium, 14-18 October 1974, Champaign, Ill.

B. Personnel

1. Mr. Yean Lee, Ph.D. Candidate
2. Mr. Duane D. Harding, Ph.D. Candidate
3. Mr. Hsiao-Ming Hsu, Ph.D. Applicant
4. Mr. Nolan Doesken, Student Assistant
5. Mr. Andrew Yagle, Student Assistant